

A Multifaceted Benchmarking of Synthetic Electronic Health Record Generation Models

Authors:

Chao Yan^{1,*}, Yao Yan^{2,*}, Zhiyu Wan^{1,*}, Ziqi Zhang³, Larsson Omberg², Justin Guinney^{4,5}, Sean D. Mooney^{4,#}, Bradley A. Malin^{1,3,6,#}

Affiliations:

¹Department of Biomedical Informatics, Vanderbilt University Medical Center, Nashville, TN

²Sage Bionetworks, Seattle, WA

³Department of Computer Science, Vanderbilt University, Nashville, TN

⁴Department of Biomedical Informatics and Medical Education, University of Washington, Seattle, WA

⁵Tempus Labs, Chicago, IL

⁶Department of Biostatistics, Vanderbilt University, Nashville, TN

*co-1st authors

#co-corresponding/senior authors

Corresponding authors:

Bradley A. Malin, Ph.D.

Email: b.malin@vumc.org

Address: Suite 1475, 2525 West End Ave, Nashville, TN, USA, 37203

Sean D. Mooney, Ph.D.

Email: sdmooney@uw.edu

Address: 850 Republican St, Seattle, WA, USA, 98109

ABSTRACT

Synthetic health data have the potential to mitigate privacy concerns when sharing data to support biomedical research and the development of innovative healthcare applications. Modern approaches for data generation based on machine learning, generative adversarial networks (GAN) methods in particular, continue to evolve and demonstrate remarkable potential. Yet there is a lack of a systematic assessment framework to benchmark methods as they emerge and determine which methods are most appropriate for which use cases. In this work, we introduce a generalizable benchmarking framework to appraise key characteristics of synthetic health data with respect to utility and privacy metrics. We apply the framework to evaluate synthetic data generation methods for electronic health records (EHRs) data from two large academic medical centers with respect to several use cases. The results illustrate that there is a utility-privacy tradeoff for sharing synthetic EHR data. The results further indicate that no method is unequivocally the best on all criteria in each use case, which makes it evident why synthetic data generation methods need to be assessed in context.

INTRODUCTION

The analysis of large quantities of data derived from electronic health records (EHRs) has supported a number of important investigations into the etiology of disease, personalization of medicine, and assessment of the efficiencies and safety in healthcare administration¹⁻³. Mounting evidence suggests that broader data sharing would ensure reproducibility, as well as larger and more robust statistical analysis^{4,5}. Yet EHR data are rarely shared beyond the borders of the healthcare organization that initially collected the data. This is due to a number of reasons, some of which are technical, others of which are more social in their nature. In particular, the privacy of the patients to whom the data correspond is often voiced as a reason for not sharing such data^{6,7}.

Over the past several years, the notion of synthetic versions of EHR data has been proposed as a solution for broader data sharing^{8,9}. While synthetic data are not novel in principle, recent advances in machine learning have opened up new opportunities to model complex statistical phenomena within such data, which could support a variety of applications⁸. For instance, detailed synthetic data could make it easier to develop techniques for clinical decision support, as well as prototype automated research workflows¹⁰. At the same time, synthetic data can sever the direct relationship with the real patient records upon which they are based, thus mitigating privacy concerns^{9,11}. As a result, a growing set of research initiatives have developed, or are considering the use of, synthetic data sharing, including the National COVID Cohort Collaborative (N3C)¹² (<https://covid.cd2h.org/n3c>) supported by the U.S. National Institutes of Health and the Clinical Practice Research Datalink¹³ (<https://cprd.com/synthetic-data>) sponsored by the U.K. National Institute for Health and Care Research.

While various synthetic EHR data generation techniques have been proposed, generative adversarial networks (GANs) have gained a substantial amount of attention, with their potential illustrated for a wide range of applications^{8,14,15}. Informally, a GAN is composed of two neural networks that evolve over a series

of training iterations: 1) a generator that attempts to create realistic data and 2) a discriminator that aims to distinguish between synthetic and real data¹⁶. Iteratively, the generator receives feedback from the discriminator, which it leverages to tune its network to more effectively imitate the real data. Unlike traditional data synthesis approaches, which either explicitly model clinical knowledge or make assumptions about the relationships between features^{17,18}, models built through GANs circumvent these challenging issues by directly learning complex relationships from multi-dimensional data.

The field has advanced rapidly; however, there has been little attention paid to benchmarking, which is a concern for several reasons. First, there is a lack of consensus on the evaluation metrics that should be applied to assess synthetic EHR data. Yet this is critical to comprehensively compare and contrast candidate synthesis models. While several investigations have demonstrated the superiority of new GAN models over existing models, the comparisons are not systematic and are susceptible to the self-assessment trap¹⁹ in that the model developers benchmark their own models. Second, there is a wide range of use cases for synthetic data, each with their own set of priorities regarding what aspects of the data should be preserved. Most publications on EHR data synthesis neglect the use case, such that it is unclear what conditions are ideal for the simulation model. Third, prior evaluations have typically focused on the simulation and evaluation of a single execution, such that only one synthetic dataset is generated by each model^{20,21}. This is problematic because GAN models are often associated with unstable training trajectories, which can lead to quite different models and inconsistencies in the quality of the generated data^{15,22,23}.

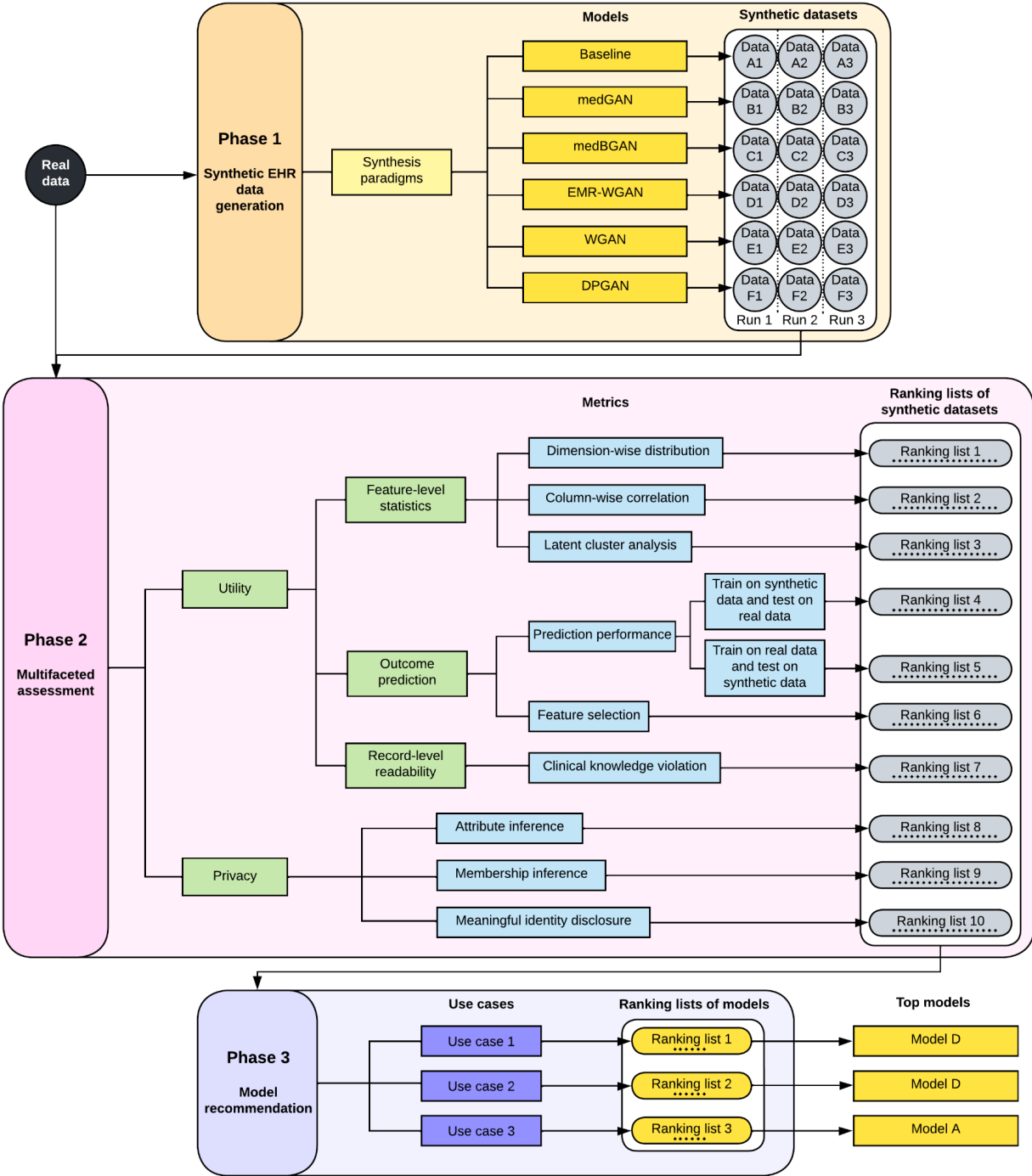


Figure 1. An overview of the synthetic EHR data generation benchmarking framework. The framework is composed of three phases: 1) Synthetic EHR data generation, 2) a multifaceted assessment process, and 3) a use case-specific model recommendation process. In Phase 1, given a synthesis paradigm and the real data, we generate multiple (specifically, three in our experiments) synthetic datasets using each EHR data generation model. In Phase 2, each generated synthetic dataset is assessed and assigned a value in terms of each assessment metric. Afterward, all synthetic datasets will be ranked according to their values in terms of each metric. In Phase 3, for each use case, we assign a weight to each metric and convert multiple (specifically, ten in our experiments) ranking lists of synthetic datasets into one ranking list of models. Finally, the top model in the ranking list for each use case is recommended.

In this paper, we introduce a benchmarking framework to evaluate GAN models for EHR synthesis (Fig.

1). We focus specifically on structured EHR data²⁴, as this type of data has supported numerous clinical association and outcome prediction studies. There are several specific contributions of this work:

1. We incorporate a complementary set of data utility and privacy metrics into the benchmarking framework to enable a systematic evaluation of synthesis models.
2. We introduce a novel rank-based scoring mechanism that converts scores from individual metrics into the final score of a model. This mechanism enables tradeoffs between competing evaluation metrics.
3. To enable broad reuse, the framework accommodates multiple aspects of complexity from GAN-based synthesis, including various data types in real data (e.g., categorical and continuous feature representations), different data synthesis paradigms (i.e., the way real data is applied to train generative models), and the inconsistent quality of synthesized data by GAN models.
4. We use EHR data from two large academic medical centers in the United States to benchmark the state-of-the-art GAN models. We demonstrate the flexibility and generalizability of the framework through contextualized construction of concrete use cases, where synthetic EHRs already (or have the potential to) provide support.
5. Our findings show that no model is unequivocally the best on all criteria in each use case for each dataset. This result clearly illustrates why synthetic data generation models need to be systematically assessed in the context of their use case before their application.

RESULTS

Benchmarking framework

The benchmarking framework focuses on two perspectives — utility and privacy (Fig. 1). Table 1 summarizes the metrics incorporated into the Multifaceted assessment phase of the benchmarking framework. Detailed metric descriptions can be found in Methods.

Data utility was measured using three types of criteria: 1) feature-level statistics — that is, the ability to capture characteristics of the distributions of real data - through *dimension-wise distribution*²⁵, *column-wise correlation*²⁶, and *latent cluster analysis*²⁷; 2) outcome predictions - that is, the ability to train and evaluate machine learning models - as measured by *model performance*²⁸ and *feature selection*; and 3) record-level readability, in terms of the ability to avoid generating individual records that violate clinical knowledge as measured by *clinical knowledge violation*. All of these metrics, save for *feature selection* and *clinical knowledge violation*, were drawn from prior publications. Notably, the three metrics for feature-level statistics differ in the distributions considered and correspond to the marginal distribution, the correlation between two features, and the joint distribution of all features, respectively.

Data privacy was assessed through three metrics, each representing a distinct attacker model: 1) attribute inference²⁵, in which unknown attribute values of interest are predicted from a set of real attribute values, 2) membership inference²⁵, which indicates whether a real record was used to train a generative model, and 3) meaningful identity disclosure²⁹, in which the identity and sensitive attributes of a patient’s record are detected as being part of in the real dataset. The privacy risks were measured under the typical assumption about an attacker’s knowledge. Specifically, it was assumed that the attacker has access to synthetic data, but not the generative models^{20,25,30}. It should be noted that we will mainly use the term attribute (instead of feature) in the context of privacy risk to be consistent with the privacy literature. Additionally, we will use *record* to denote the data for a patient.

Table 1. A summary of the metrics in the framework. The direction of the values indicates if a higher (↑) or lower (↓) value is better.

	Metric	Summary	Direction
Utility	Dimension-wise distribution	The ability to capture marginal feature distributions in real data. This is calculated as the average of the absolute prevalence differences (APD) for binary features and the average of the Wasserstein distances (AWD) for continuous features between real and synthetic datasets.	↓
	Column-wise correlation	The ability to capture the relationship between two features in real data. This is calculated as the average of the cell-wise absolute differences of the Pearson correlation coefficient matrices derived from real and synthetic datasets.	↓
	Latent cluster analysis	The ability to capture the joint distribution of all features in real data. This is calculated as the deviation of a synthetic dataset in the underlying latent space from the corresponding real dataset in terms of unsupervised clustering.	↓
	TSTR Model performance	The ability to approximate the performance of the downstream task of machine learning model development. Given an outcome prediction task, this is calculated as the model performance, typically the area under the receiver operating characteristics curve (AUROC), in the scenario of training on synthetic dataset and testing on real dataset (TSTR).	↑
	TRTS Model performance	The ability to generate convincing and realistic data records for different labels. Given an outcome prediction task, this is calculated as the model performance, typically the AUROC, in the scenario of training on real dataset and testing on synthetic dataset (TRTS).	↑
	Feature selection	The ability to support model interpretability in downstream tasks. This is calculated as the number of shared important features for models trained on a synthetic dataset and the corresponding real dataset.	↑
	Clinical knowledge violation	The ability to learn the clinical knowledge at the patient level. This is calculated as the proportion of generated records that violate clinical knowledge derived from the real dataset (e.g., the synthetic records for male patients are frequently associated with pregnancy diagnosis codes).	↓
Privacy	Attribute inference	The adversary’s ability to infer sensitive attributes of a targeted record. Given demographics and some sensitive attributes of a targeted record, this is calculated as the weighted sum of F1 scores of the inferences of other sensitive attributes.	↓

Membership inference	The adversary’s ability to infer the membership of a targeted record. Given a set of attributes of a targeted record, this is calculated as the F1 score of the inference based on Euclidean distances between the targeted record and all synthetic records.	↓
Meaningful identity disclosure	The adversary’s ability to identify synthetic records with meaningful attributes. Given a population dataset with identities, this is calculated as the adjusted re-identification risk considering the linkage between the synthetic dataset and the real dataset, the linkage between the synthetic dataset and the population dataset, and the rareness of each sensitive attribute in the real dataset.	↓

Prior studies into synthetic EHR data compared models using only a single training of the generator. Yet this can lead to a less reliable evaluation because GAN models can be unstable relative to training (leading to models with large differences in parameters)^{15,22}, making it hard to yield synthetic datasets of consistent data quality^{31–33}. In this work, we integrated a mechanism into the framework that involves training multiple models and generating data from each to capture variations in models and baking biases into model comparison (Synthetic EHR data generation phase in Fig. 1). Specifically, we performed model training and synthetic data generation five times for each model. We then selected the three datasets that best preserved the dimension-wise distribution of real data for the benchmarking analysis. We rely upon this metric to filter synthetic datasets because it is a basic utility measure and provides face-value evidence of the usability of synthetic data. In doing so, we drop the synthetic datasets that poorly captured the first-moment statistics of individual features.

We designed a novel ranking mechanism that scores each model based on the results of three independently generated datasets. Specifically, for each metric, we calculated the metric scores for all of the datasets generated by all candidate models. Next, for each metric, we ranked the synthetic datasets - with smaller ranks denoting better performance of a dataset on the given metric. For each metric, we defined the average of the ranks of each model’s three synthetic datasets as the *rank-derived score* on this metric. Thus, there were ten lists of ranks and rank-derived scores, one for each metric. The *final score* for a model was the

weighted sum of the rank-derived scores, where the weights were tailored to the specific use case in the Model recommendation phase. An example of this process is provided in Methods.

We used this framework to evaluate five EHR synthetic data generation models based on GANs⁸: 1) medGAN²⁵, 2) medBGAN³⁴, 3) EMR-WGAN²⁰, 4) WGAN³⁴, and 5) DPGAN³⁵. Additionally, we incorporated a baseline approach that randomly samples the values of features based on the marginal distributions of the real data to complement the scope of benchmarking in terms of the variety of model behavior. We refer to this approach as the sampling baseline, or *Baseline*. Interestingly, as our results illustrate, this approach outperformed the GAN models in practical use cases. Details for the models are provided in Methods.

Datasets

We performed our benchmarking using EHR data from two large academic medical centers in the United States, the University of Washington (UW) and Vanderbilt University Medical Center (VUMC). Table 2 provides summary characteristics for the data. The UW dataset was introduced in a public DREAM Challenge for mortality prediction³⁶. It includes 2,665 features from 188,743 patients who visited UW health system between January 2007 to February 2019. By contrast, the VUMC dataset includes 2,592 features from 20,499 patients who tested positive for COVID-19 at an outpatient visit from March 2020 to February 2021.

Table 2. The characteristics of the benchmarking datasets. x, y, z represents the first quartile, median, and third quartile. $x \pm y$ represents the mean and one standard deviation. $x\% y$ represents that the percentage of y patients is $x\%$ among all patients.

	UW Dataset		VUMC Dataset	
Age	-		26.0, 40.3, 55.8	41.0 \pm 18.7
Race				
White	69.9%	131,830	65.2%	13,366
Black	7.9%	14,956	8.8%	1,794
Asian	9.4%	17,646	1.9%	384
American Indian or Alaska Native	1.5%	2,836	0.0%	42
Pacific Islander	0.8%	1,563	0.0%	0
Unknown	10.5%	19,912	24.0%	4,913
Gender				
Male	45.3%	85,490	43.9%	8,990
Female	54.7%	103,253	56.1%	11,509
Medical features for generation				
<i>Binary features</i>				
# of unique codes	2,662		2,581	
Diagnosis (Phecode)	1,736		1,269	
Procedure (Category)	66		67	
Medication (RxNorm Ingredient)	860		1,245	
# of unique codes per patient	13.0, 30.0, 51.0	36.8 \pm 31.3	6.0, 21.0, 59.0	45.3 \pm 63.6
<i>Continuous features</i>				
Diastolic Pressure	-		68.0, 75.0, 82.0	75.0 \pm 10.7
Systolic Pressure	-		114.0, 124.0, 136.0	125.3 \pm 15.9
Pulse	-		77.3, 90.0, 104.3	91.4 \pm 18.6
Temperature	-		36.8, 37.1, 37.7	37.3 \pm 0.6
Pulse Oximetry	-		95.1, 97.1, 99.0	97.1 \pm 2.1
Respirations	-		16.0, 18.0, 23.9	19.6 \pm 4.4
Body Mass Index	-		24.4, 30.3, 38.1	31.3 \pm 8.7
Data split for prediction				
<i>Training data</i>				
Positive label	3.8%	4,966	3.8%	541
Negative label	96.2%	127,158	96.2%	13,808
<i>Evaluation data</i>				
Positive label	3.8%	2,129	4.2%	260
Negative label	96.2%	54,490	95.8%	5,609

Data utility

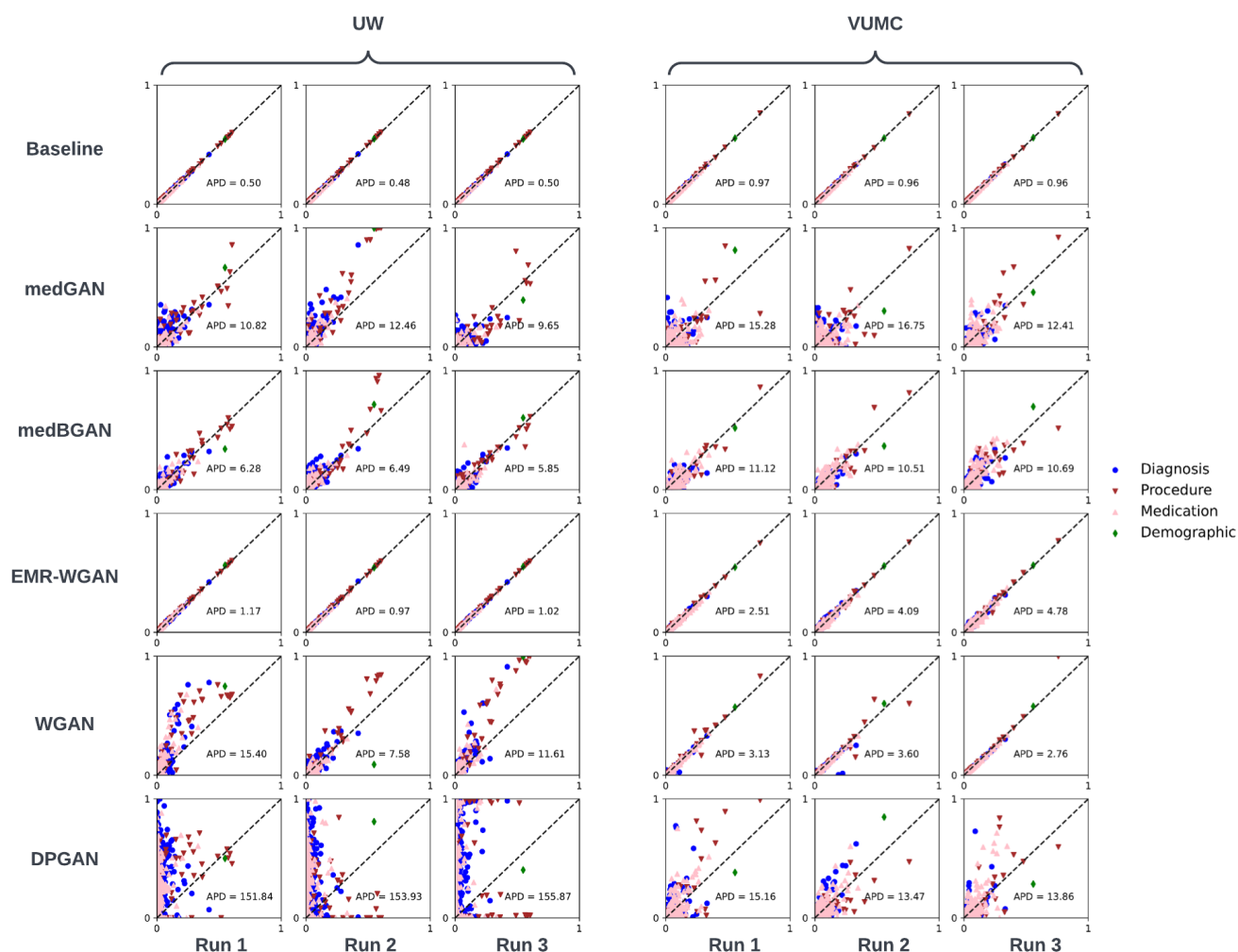


Figure 2. Dimension-wise distribution for the UW (left) and VUMC (right) datasets. Here, the x- and y-axes correspond to the prevalence of a feature in real and synthetic data, respectively. The results for three independently generated synthetic datasets are shown for each candidate model. Feature dots on the dashed diagonal line correspond to the perfect replication of prevalence.

Fig. 2 depicts the prevalence of categorical features for the real and synthetic datasets. It can be seen that Baseline consistently achieved the most similar marginal distributions to real data for both datasets, as it achieves the lowest APD of all synthesis models. Among the GAN synthetic datasets, those generated by EMR-WGAN achieved a clear pattern for both UW and VUMC datasets in which all binary features were closely distributed along the diagonal line, suggesting a strong capability of retaining the first-moment statistics in the real data. By contrast, medBGAN, medGAN, and DPGAN (in descending order of APD) were less competitive, exhibiting a tendency to deviate from the marginal distribution in real data. For the

VUMC dataset, the synthetic datasets from WGAN exhibited a similar pattern to those generated by EMR-WGAN in terms of APD. Yet for the UW dataset, WGAN achieved a substantially higher APD than EMR-WGAN. DPGAN, which enforced a differential privacy constraint on WGAN, led to heavier deviations from the marginal distribution in real data. Additionally, all models, except for WGAN and DPGAN, achieved higher APD for the UW dataset than for the VUMC dataset.

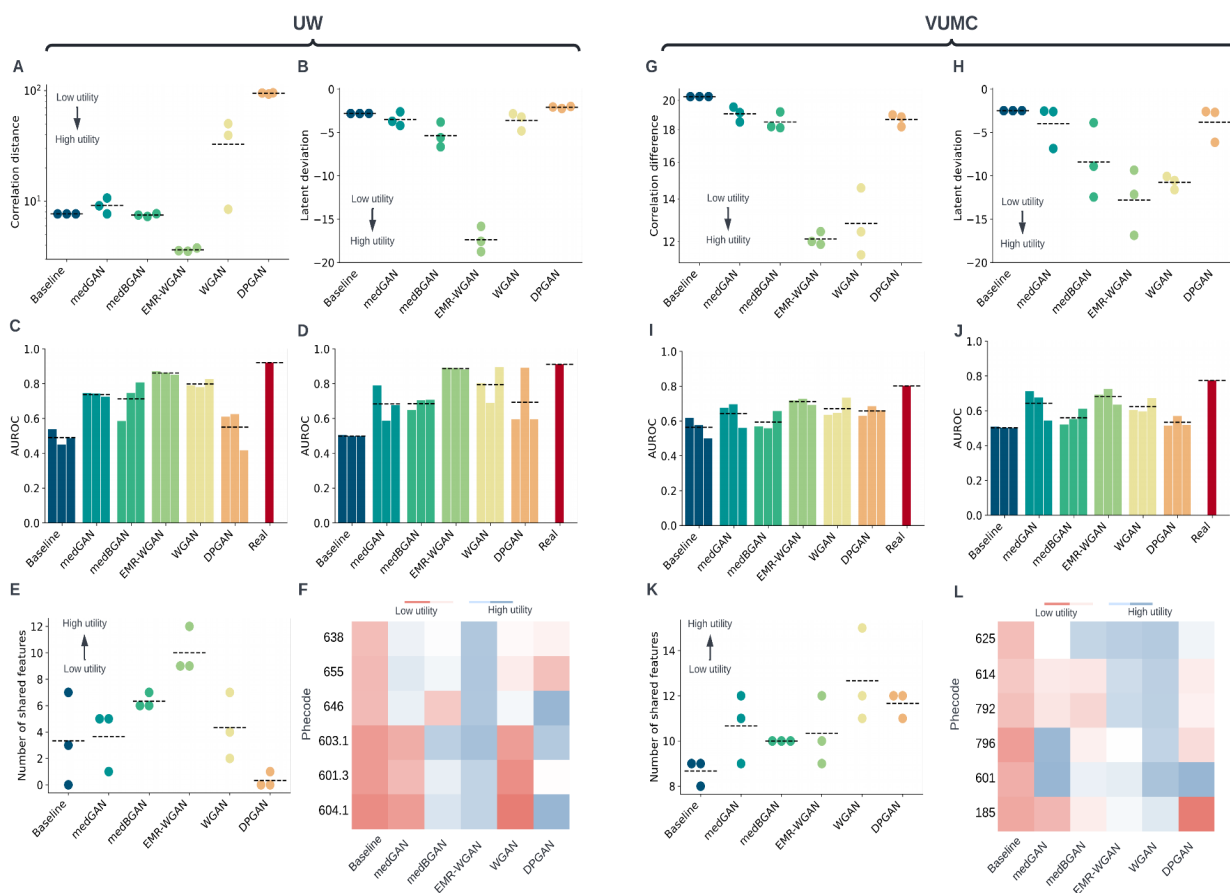


Figure 3. Data utility for the UW (left, A-F) and VUMC (right, G-L) datasets. (A,G) Column-wise correlation; (B,H) Latent cluster analysis; (C,I) TSTR Model performance for training on synthetic data; (D,J) TRTS Model performance; (E,K) The number of top k features in common (25 for UW and 20 for VUMC); (F,L) Clinical knowledge violation for gender-specific phecodes. Log scale is applied to the y-axis in A and G. The heatmaps correspond to the ratio of clinical knowledge violations in gender (blue = low value; red = high value). A dashed line indicates the mean value across three synthetic datasets. (Phecode definitions: 625: Symptoms associated with female genital organs; 614: Inflammatory diseases of female pelvic organs; 792: Abnormal Papanicolaou smear of cervix and cervical HPV; 796: Elevated prostate-specific antigen; 601: Inflammatory diseases of prostate; 185: Prostate cancer; 638: Other high-risk pregnancy; 655: Known or suspected fetal abnormality; 646: Other complications of pregnancy NEC; 603.1: Hydrocele; 601.3: Orchitis and epididymitis; 604.1: Redundant prepuce and phimosis/BXO)

Fig. 3 depicts six data utility metrics for the real and synthetic datasets. EMR-WGAN exhibited the highest average utility for the UW dataset for all individual utility metrics except for dimension-wise distribution (Fig. 3A-3F). EMR-WGAN was also the best model according to four (Fig. 3G-3J) of the six metrics for the VUMC dataset. For the other two metrics (i.e., feature selection and clinical knowledge violation), WGAN achieved the best performance, which suggests it is more adept at model interpretability and patient-level record readability (Fig. 3K-3L). By contrast, for the VUMC dataset, Baseline consistently had the worst average utility (Fig. 3G-3L). Also, for the UW dataset, Baseline was one of the two worst performing models for five metrics (Fig. 3B-3F). DPGAN also performed poorly as it can be seen that it was associated with the lowest utility for the UW dataset in terms of column-wise correlation, latent cluster analysis, and feature selection. The results (Fig. 5A-5B) were generally consistent with the mean metric score (as indicated by the dashed lines and colored cells in Fig. 3) derived from synthetic datasets to rank models. However, this finding did not hold true when there was a large variance in a model's utility. For example, medGAN outperformed medBGAN in terms of average AUROC when training on synthetic and testing on real data (Fig. 3C), but medBGAN achieved a better rank-derived score (Fig. 5A) because two datasets generated by medBGAN outperformed all datasets generated by medGAN.

Data privacy

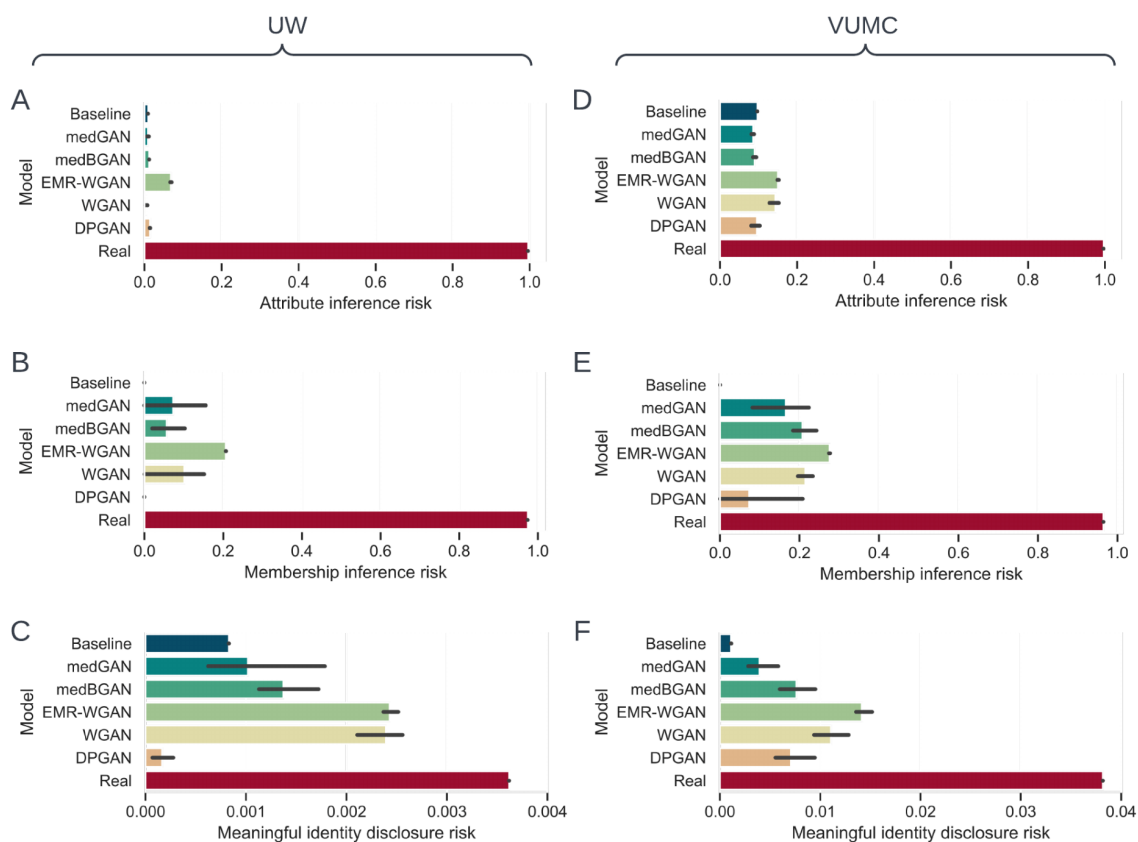


Figure 4. Average privacy risk of the synthetic versions of the UW (A-C) and VUMC (D-F) datasets. (A,D) Attribute inference risk; (B,H) Membership inference risk; (C,I) Meaningful identity disclosure risk. The risk associated with the real data are shown in the bottom red bars. The 95% confidence intervals are marked as thin horizontal black lines.

Fig. 4 depicts three data privacy metrics for the real and synthetic datasets. All synthetic datasets achieved a lower privacy risk than the real data. In terms of membership inference and meaningful identity disclosure, Baseline posed the lowest average risk except that DPGAN achieved the lowest average meaningful identity disclosure risk for the UW dataset. In terms of attribute inference (Fig. 4A and Fig. 4D), WGAN achieved the lowest average risk for the UW dataset and medGAN achieved the lowest average risk for the VUMC dataset. On the other hand, EMR-WGAN posed the highest average risk on all privacy metrics. However, even the highest risks posed by EMR-WGAN in our experiments for each privacy metric (i.e., 0.152 for the attribute inference risk, 0.276 for the membership inference risk, and 0.015 for the meaningful identity disclosure risk) can be regarded as low risk if we segment the range of risk from 0 to 1 equally into three

categories (i.e., low, median, and high) in which the low risk category means the risk is lower than 0.333. Note that Zhang et al.²⁰ used the highest risk among risks posed by either medBGAN or WGAN as the threshold for both the attribute inference risk and the membership inference risk (i.e., 0.152 and 0.242, respectively, for our experiments). From this perspective, only EMR-WGAN for the VUMC dataset has a slightly higher membership inference risk than the threshold. In addition, El Emam et al.²⁹ used 0.09 as the threshold for the meaningful identity disclosure risk to determine whether a synthetic dataset is risky, which is much higher than 0.015, under the guidelines from the European Medicines Agency³⁷ and Health Canada³⁸ for the sharing of clinical data, whereas some custodians used 0.333 as the threshold^{39,40}.

Utility Privacy Tradeoff

Figs. 5A and 5B provide a summary of models' rank-derived scores with respect to each utility and privacy metric. The privacy-utility tradeoff in both datasets is evident. A generative model associated with a higher utility (e.g., EMR-WGAN) usually had a lower privacy score, whereas a model associated with a higher privacy score often had lower utility, as illustrated in Baseline for the VUMC dataset and DPGAN for the UW dataset. The other models, which exhibited a moderate utility ranking, were often associated with a moderate privacy ranking as well. This phenomenon generally holds true for all of the models tested.

To illustrate how the benchmarking metrics complement each other, we investigated their pairwise correlation. In doing so, a strong correlation indicates that two metrics provide similar rank-derived scores across models and two real datasets, whereas a weak correlation implies that the two metrics complement each other by discriminating model assessment. Fig. 5C depicts a heatmap of the rank-derived scores (in Fig. 5A-5B) across all models for the VUMC and UW datasets. There are several notable findings. First, the privacy-utility tradeoff is evident from the fact that all pairs of utility and privacy metrics were negatively correlated. Second, numerous weak correlations were observed in the utility metrics, including a very weak negative correlation between TRTS Model performance and dimension-wise distribution. In

particular, the performance of synthesis models on dimension-wise distribution was weakly correlated with the model prediction performance and clinical knowledge violation metrics. Yet, there was a relatively strong correlation (correlation coefficient = 0.89) between column-wise correlation and latent cluster analysis. Third, from a privacy perspective, attribute inference exhibited weak correlations with the other two privacy metrics, whereas the membership inference rankings were strongly correlated with meaningful identity disclosure (correlation coefficient = 0.88). With only 2 (out of 45) metric pairs strongly correlated (correlation coefficient > 0.85), the results indicate that the metrics are complementary and belong in the framework.

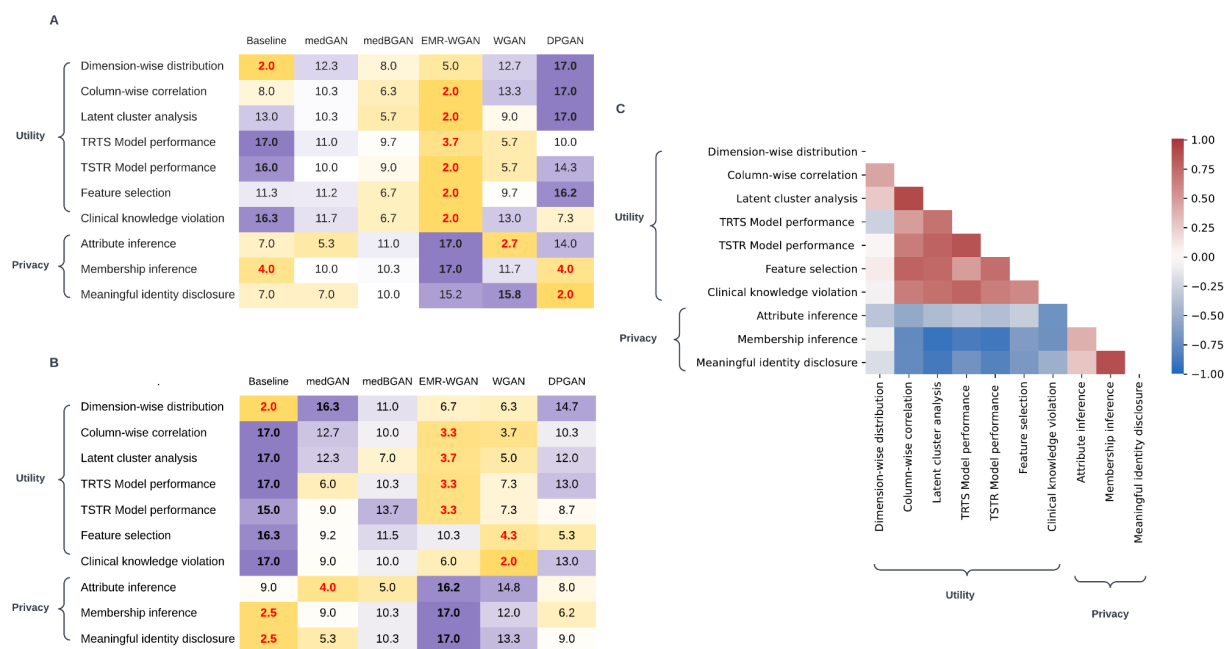


Figure 5. Rank-derived scores of synthesis models and metric correlations. (A) Rank-derived scores on synthetic data generated using UW data; (B) Rank-derived scores on synthetic data generated using VUMC data; (C) A heatmap of the Pearson correlation coefficients for pairwise metrics on the rank-derived scores across all candidate models for the two real datasets (UW and VUMC). The best (i.e., lowest rank) and worst scores for each metric are in bold red and black font, respectively.

Model selection in the context of use cases

Generative model benchmarks need to be contextualized through specific use cases, where different uses of the synthetic data will have different priorities when it comes to the different measures in the framework.

In the Model recommendation phase, we apply three example use cases to illustrate the process and select

the most appropriate synthetic data generation model: 1) education, 2) medical AI development, and 3) systems development (as detailed in Methods). Each use case is associated with a different set of weights for the utility and privacy metrics. We adjusted the weights assigned to the ranking results from individual metrics for each use case according to their typical needs. For example, the utility weights for the first-moment statistics, medical concept correlations, and patient-level clinical knowledge were set higher in the education scenarios than in other use cases, whereas privacy risks were of less concern than in the systems development and medical AI development use cases. By contrast, medical AI development provides greater emphasis on the metrics for model development and interpretability than the other two use cases. The systems development use case places a greater emphasis on privacy risks and data sparsity to support function and data flow testing.

Table 3. Overall rank of generative models for the use cases in the Model recommendation phase. Model ranks were based on the benchmarking framework scores (in parenthesis). The fact that DPGAN and EMR-WGAN have the same score for the VUMC dataset in the Medical AI Development use case is due to precision loss instead of an actual tie.

Use Case	Dataset	Overall Model Rank					
		1	2	3	4	5	6
Education	UW	EMR-WGAN (4.9)	medBGAN (7.7)	Baseline (9.1)	medGAN (10.6)	WGAN (11.1)	DPGAN (13.6)
	VUMC	WGAN (6.1)	EMR-WGAN (7.3)	medBGAN (10.3)	DPGAN (10.9)	Baseline (11.1)	medGAN (11.3)
Medical AI Development	UW	EMR-WGAN (6.5)	medBGAN (8.6)	WGAN (8.9)	medGAN (9.6)	Baseline (11.1)	DPGAN (12.4)
	VUMC	WGAN (8.1)	DPGAN (8.7)	EMR-WGAN (8.7)	medGAN (8.9)	medBGAN (11.0)	Baseline (11.7)
Systems Development	UW	Baseline (6.7)	medBGAN (8.9)	medGAN (9.5)	EMR-WGAN (10.0)	WGAN (10.7)	DPGAN (11.2)
	VUMC	Baseline (6.9)	WGAN (9.4)	medBGAN (9.6)	medGAN (9.7)	DPGAN (10.0)	EMR-WGAN (11.4)

Table 3 summarizes the final ranking results for the generative models based on the use cases. It can be seen that EMR-WGAN and WGAN best support education and medical AI development, respectively. By contrast, sampling-based Baseline was best for systems development. It is notable that, in the systems development use case, EMR-WGAN and DPGAN achieved the lowest rankings for the VUMC and UW, respectively. Additionally, DPGAN demonstrated ranking scores that were no better than WGAN on all of the six scenarios considered (use case by dataset).

Synthesis paradigms

The benchmarking framework was designed to accommodate the need to incorporate different data synthesis paradigms regarding the outcome variable of interest (e.g., the 21-day hospital admission post COVID-19 positive testing and six-month mortality in general) as part of the benchmarking. This is because the selection of synthesis paradigms can make an impact on the utility and privacy of synthetic data. We tested two synthesis paradigms: 1) *combined synthesis paradigm* (Fig. 6C) and 2) *separate synthesis paradigm* (Fig. 6D). See Methods for details.

We observed that the separate synthesis paradigm demonstrated several advantages over the combined synthesis paradigm. First, the separate paradigm tended to achieve better utility on the dimension-wise distribution and outcome prediction metrics, while sustaining no greater privacy risks (Supplementary Fig. A.1-3, Supplementary Table A.3). In all use cases, the separate synthesis paradigm outperforms the combined synthesis paradigm for all six models (Supplementary Table A.4), save for two situations: 1) the educational use case, where the combined synthesis paradigm led to better performance than the separate synthesis paradigm for DPGAN, and 2) the system development use case, where the combined synthesis paradigm led to better performance than the separate synthesis paradigm for medGAN.

The raw values for each evaluation metric are provided in Supplementary B.

DISCUSSION

The framework introduced in this work provides a mechanism to determine which EHR data synthesis models are most appropriate for which use case for a given dataset. The framework can further be applied to guide the development of new synthesis models by enabling greater consistency in evaluations. There are multiple aspects worth discussing.

Model comparison

The benchmarking results with the UW and VUMC datasets yielded several notable findings. First, EMR-WGAN consistently performs well for the majority of utility metrics (Fig. 5 A-B and Supplementary Table A.1). This benefit is clearly due to a sacrifice in privacy, as this method also consistently exhibited the greatest privacy risks. Second, the inverse is true for Baseline, in that it achieves low privacy risks at the expense of low utility (except for dimension-wise distribution) (Fig. 5A-B and Supplementary Table A.1). This is not surprising because its sampling strategy neglects the joint distribution of the real data. Third, DPGAN, which adds a small amount of noise to WGAN, achieved a similar or worse ranking than WGAN (Table 3 and Supplementary Table A.4). This implies that, at least for the settings considered in this study, there is not much benefit in incorporating differential privacy into the synthetic data generation process.

In addition, it is worth remarking that there are non-trivial differences in model performance between the UW and VUMC datasets. Notably, with respect to APD (Fig. 2), while WGAN and DPGAN perform well for the VUMC dataset, they do not for the UW dataset. This finding may stem from differences in the complexity of the joint distribution between the two real datasets. At the same time, this finding may also be an artifact of the differences in the selected synthesis paradigms. It can be seen, for instance, that the separate synthesis paradigm led to an improved feature distribution resemblance (Supplementary Fig. A.1).

Utility-privacy tradeoff

Our analysis also provides evidence of a utility-privacy tradeoff across the synthesis models. This phenomenon has been widely discussed in the data privacy literature^{41,42}, where traditional privacy-preserving approaches (e.g., generalization or suppression of sensitive information) are applied to make changes directly to the real dataset that will be shared. Yet this phenomenon is characterized by several aspects of our study on synthetic data. First, no data synthesis model is unequivocally the best for all metrics, use cases, or datasets (Fig. 5A-B and Supplementary Table A.1). Second, the overall ranks of data synthesis models differ across synthetic data use cases. For example, Baseline was the worst for Medical AI development, but was the best for System development (Table 3). Third, the evaluation metrics for data utility and privacy are negatively correlated in general (Fig. 5C). These findings highlight why is critical to contextualize the comparison of EHR synthesis models through concrete use cases.

In investigating how evaluation metrics relate to each other, we observed two correlations that are stronger than others (Fig. 5). First, there was a strong positive correlation between column-wise correlation and latent cluster analysis, which suggests that, if a GAN-based model retained correlations between features in real data, it was likely able to represent the joint distribution of the real data as well. This is because GANs do not explicitly learn from local feature correlations, but rather focus on global patterns. Second, unsurprisingly, there was a strong relationship between membership inference and identity disclosure. When a synthetic record has a high meaningful identity disclosure risk, it likely contains values that are very similar to a real record on a substantial portion of its sensitive attributes. Similarly, when a synthetic record has a high membership inference risk, there is a real record in the training data that it looks very similar to. Thus, it is likely that the two records match their quasi-identifiers and contribute to a high meaningful identity disclosure risk. However, these two observations do not imply that there exists redundancy in metrics because 1) they measure clearly different data characteristics, 2) this observation might not generalize to other GANs or non-GAN models that can lead to reduced correlations, and 3) the correlation coefficients (<0.9) are still deemed imperfect correlations.

Knowledge violation

We observed that all models induced some level of knowledge violation, while the rates of violation at which the occurrence transpired differ between the methods. For instance, we observed a non-trivial number of violations in commonsense sex-disease relationships for all models (Fig. 3F, 3L). For instance, over 50% of the synthetic records with prostate cancer diagnosis code generated by DPGAN are associated with a generated “Female” gender. This phenomenon implies that GAN models are unable to perfectly recognize and learn from the record-level knowledge in EHR. Although such violations can be partially resolved through a post-hoc editing process before data are shared, this phenomenon suggests that further research is necessary for the development of synthesis methods, such as embedding constraints of violations as a penalty into the learning process²¹.

Limitations

Despite the merits of this study, there are several limitations that provide opportunities for future improvement. First, the evaluation metrics we incorporated into the benchmarking framework do not necessarily represent the entire metric universe for synthetic data assessment. We aimed to cover the key characteristics of synthetic data by introducing representative metrics and did not incorporate every related metrics that could create redundancy. However, the framework can readily be extended to incorporate new utility and privacy metrics as they are introduced.

Second, this study relied upon a handful of use cases to assess the synthesis models and interpret the results that do not cover the gamut of all possible applications. As a result, the weight profiles applied to the measures in the evaluation may not sufficiently represent the space. There is clearly an opportunity to explore how changing the weights influences model rankings. In particular, we neglected scenarios where the privacy risks were already sufficiently low, such that the synthetic datasets should only be assessed for their utility. Yet, the challenge in this scenario is that there is no clear consensus on what an acceptable

privacy risk threshold for synthetic data is²⁹. In this respect, we believe that further discussion and deliberation on legal standing and policy making is needed to inform the benchmarking framework⁴³. On the other hand, when the goal of data synthesis is to support data augmentation^{44,45} (rather than data sharing), where the limited volume and representativeness of the real data that are now available can be addressed to boost the effectiveness of medical AI algorithms⁴⁶⁻⁴⁸, maintaining data utility becomes the primary goal of synthetic data generation. The benchmarking framework can provide support to data augmentation by ruling out privacy components by setting the weights of the related metrics to zero and incorporating new metrics, such as training on real and synthetic data testing on real data.

Third, the introduced benchmarking framework was specifically designed for contrasting models that generate structured EHR data. We believe that other data types in EHRs, such as longitudinal medical events, unstructured clinical notes, and medical images, are also valuable for data synthesis such that building corresponding benchmarking frameworks is critical as models emerge. The development of these frameworks requires incorporating new evaluation metrics that are specific to the nature of the data components. However, we believe our ranking strategy will still be reusable.

Fourth, we considered only a subset of GAN models for demonstration purposes. In doing so, we excluded models that were developed to resolve deficiencies in EHR synthesis that arise in specific applications. For instance, we did not include MC-medGAN, which allows for a better representation of multi-category features⁴⁹; CorGAN, which was designed to represent correlations between physically adjacent features⁵⁰; and HGAN, which considers constraints between features²¹, and others that made minor adjustments to core GAN architecture.

Finally, we aimed to use consistent parameterizations across the GAN implementations when they incorporated the same technical mechanism (e.g., the size of a deep network) while respecting the original implementations of all methods. However, the datasets we used in this study were not the same as those

relied upon in the development of these methods. As a consequence, it is possible that the parameter settings we relied upon might not be optimal. Thus, a more extensive set of experiments is needed to investigate the generalizability of our observations on benchmarking results.

METHODS

The Institutional Review Boards at Vanderbilt University Medical Center and the University of Washington approved this study under IRB#211997 and 00011204, respectively.

Dataset

University of Washington (UW). This dataset comes from the general population at UW Medicine enterprise data warehouse, which manages EHR data from more than 60 medical sites across the UW Medicine system including the University of Washington Medical Center, Harborview Medical Center, and Northwest Hospital and Medical Center. Specifically, data from January 2007 to February 2019 for patients with at least 10 visits within two years prior to the date of the latest recorded visit were used. This dataset includes diagnoses, medications, procedures, and an indication of if the patient died within six months after the final visit date of the patient⁵¹. This dataset covers 188,743 patients.

Vanderbilt University Medical Center (VUMC). This dataset corresponds to a cohort of COVID-19 positive patients who visited VUMC. Specifically, we selected the patients who tested positive (via a polymerase chain reaction test) in an outpatient visit before February 2021. For those who exhibited multiple positive testing results, we retained one at random. We collected the diagnoses, medications, and procedures from these patients' EHRs between 2005 and the date of the positive COVID-19 test. Additionally, the most recent readings for the seven most prevalent measures or laboratory tests prior to the selected positive testing events were included. This corresponded to *diastolic and systolic blood pressures, pulse rate, temperature, pulse oximetry, respiration rate, and body mass index*. For this dataset, the prediction task is whether a patient was admitted within 21 days of their COVID-19 test⁵². This dataset covers 20,499 patients.

To standardize data representation, we converted the categorical features, including diagnoses (encoded as International Classification of Diseases Ninth or Tenth Revision, or ICD9/10), procedures (encoded as

Current Procedural Terminology Fourth Edition, or CPT4), medications (encoded as RxNorm Drug Terminology), and demographics (gender and race), to a binary format to denote the presence (or absence) of the corresponding concepts. We followed the convention of dimensionality reduction preprocessing^{20,25,53} by 1) mapping the ICD9/10 codes into Phenome-wide Association Studies (PheWAS) codes, or phecodes, which aggregate billing codes into clinically meaningful phenotypes, 2) generalizing the CPT4 codes using a hierarchical architecture of procedures⁵⁴, and, 3) converting clinical RxNorm drugs to RxNorm drug ingredients. We represented the race of patients in a one-hot encoding format (i.e., a binary vector). We retained features with more than 20 occurrences in each dataset. After preprocessing, features in the UW dataset were all binary, whereas the VUMC dataset contained eight continuous features (namely, age and 7 laboratory tests).

Both datasets were split according to a 70:30 ratio into Training and Evaluation datasets. The Training datasets were relied upon to train synthetic data generation models while the Evaluation datasets were reserved for assessment purposes only.

GAN models for benchmarking

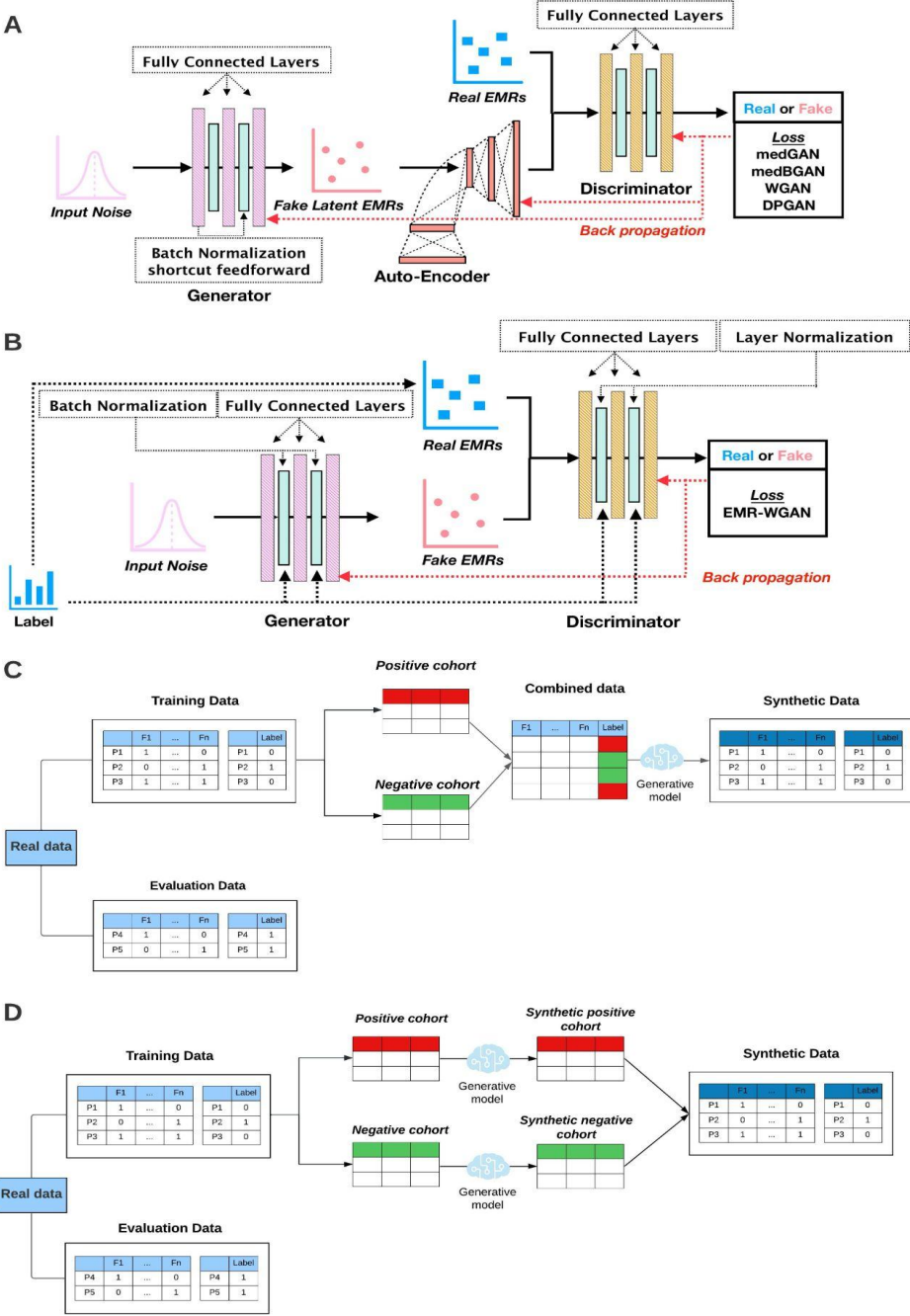


Figure 6. An architectural depiction of the deep generative models and synthesis paradigms considered in this study. The generative model architectures correspond to A) medGAN, medBGAN, WGAN, and DPGAN; and B) EMR-WGAN. The synthesis paradigms correspond to C) combined synthesis and D) separate synthesis.

Figs. 6A-B illustrate the architectures for the GAN models assessed in the benchmarking activities.

medGAN was an early attempt to leverage the power of GANs¹⁶ to synthesize individual-level EHR data²⁵. The categorical format of medical concepts created a challenging situation in learning where the GANs' approximation of the discrete data rendered the training process suboptimal. To address this issue, medGAN leveraged a pre-trained autoencoder to project the discrete representations into a compact continuous space to enhance the subsequent GANs training. Also, medGAN integrated a set of helpful learning techniques, such as batch normalization and short connection, to reduce the instability of the training process. It should be recognized that medGAN relied upon the Jensen-Shannon Divergence (JS Divergence) between the real and synthetic data distributions as the optimization objective. These designs (except for the learning objective) were inherited by several later models as shown in Figure 6A.

medBGAN was based on the same architectural designs as medGAN³⁴. To enhance training performance in terms of the quality of the synthetic data, particularly when dealing with categorical values, medBGAN replaced the loss function of the medGAN discriminator with a boundary-seeking loss function. In doing so, the generator was directed to generate synthetic data points near the decision boundary of the discriminator, which enables better generation performance particularly for categorical data.

WGAN was developed based on the observation that a learning objective adopting JS divergence can lead to diminishing gradients, which, in turn, can subsequently impede the optimization of the generator³⁴. To address this problem, WGAN incorporated Wasserstein divergence⁵⁵ into the training objective. This approach applies a Lipschitz constraint on the discriminator and ensures a more accurate characterization of the distance between two distributions. The WGAN implementation in our paper used the strategy that each of the discriminator's parameters is clipped to stay within a certain range (i.e., -0.01 - 0.01), which is referred to as parameter clipping, to satisfy the Lipschitz constraint.

DPGAN was a differentially private (DP) version of WGAN³⁵, which achieved a theoretically guaranteed privacy protection on synthetic health data via employing the differential privacy principle⁵⁶ in GAN training. It followed the differential private stochastic gradient descent (DP-SGD) mechanism in the model

training process so that it is differential private, but modified the implementation of DP-SGD by replacing gradient clipping with parameter clipping. We set ϵ to 10^4 to prevent the generation of synthetic datasets with very little to no utility.

EMR-WGAN was developed based on the observation that the autoencoder design can induce barriers during model training when working with an advanced distance measure between two distributions²⁰. EMR-WGAN had the autoencoder component removed and equipped Wasserstein divergence as its optimization objective (Fig. 6B). EMR-WGAN made several additional amendments to the architecture. First, it introduced layer normalization to the discriminator to further improve the learning performance. Second, it incorporated a gradient penalty strategy to enforce the Lipschitz constraint, which reduced the negative impact of parameter clipping on GAN's capability to approximate data distribution.

Model training and data selection

We normalized all continuous features by mapping them into a $[0,1]$ range. We trained the generative models using the normalized data and mapped the generated data back to the original space of the continuous features as a post-training step. To enable a direct comparison, all hyperparameters were assigned the same values across all models in which they resided. For instance, we used the same deep neural network architecture, learning rates, optimizers, and initialization strategies.

Given that the GAN models differed in the pattern of training loss trajectories, to ensure a fair comparison such that the optimal training status for each model can be selected, we applied several rules to select the model training endpoint. We observed that the divergence loss for medGAN and medBGAN demonstrated a pattern of fluctuation before quickly growing to a very large number. We selected the epoch right before the beginning of the increasing trend, which usually corresponded to the lowest losses. By contrast, the losses of EMR-WGAN and WGAN demonstrated a clear convergence pattern, where the losses decreased first and then stayed relatively stable; however, the quality of synthetic data can differ after loss

convergence. For both models, we examined multiple epochs from the area where the training loss converged and selected the top three synthetic datasets that demonstrated higher utility in dimension-wise distribution. For DPGAN, we observed that the loss decreased to a relatively low value and then started to fluctuate. We then selected the epoch right before fluctuation begins as the end point of training.

Multifaceted assessment

Data Utility

In earlier investigations^{8,14}, the term *utility* was defined in parallel with *resemblance* (i.e., the statistical similarity of two datasets) and was specifically used to refer to the value of real or synthetic data to support predictions. By contrast, in this work, utility is defined to cover a set of metrics, each measuring a factor to which the value of data is attributed. This is because numerous real-world use cases of synthetic data do not involve any prediction tasks, but still require the synthetic data to be useful (or have utility).

Dimension-wise distribution. The distributional distance of each feature between a real and synthetic dataset is often applied to measure data utility. In this study, we calculated the average of the absolute prevalence difference (APD) for binary features and the average of the feature-wise Wasserstein distances (AWD) for continuous features. The prevalence of a binary feature was defined as the percentage of patients who were associated with the corresponding concept in a dataset. Due to the fact that the Wasserstein distance is unbounded, for each continuous feature, we normalized the values into the range of [0,1] based on the distances derived from all synthetic datasets used for model assessment.

For a dataset with both binary (note that categorical features can be converted to binary features for synthesis) and continuous features, such as the VUMC dataset, the results of APD and AWD need to be combined into a final score. To do so, for binary features, we sum the absolute prevalence difference and, for continuous features, we sum the feature-wise (normalized) Wasserstein distances. We then averaged

the two results (i.e., divide by the total number of features). To ensure the average values are easy to read, we multiplied a factor of 1000 by the metric results, which shares the same magnitude of the number of features.

Column-wise correlation. This measure quantifies the degree to which a synthetic dataset retains the feature correlations inherent in the real data²⁶. For each pair of synthetic and real datasets, we first computed the Pearson correlation coefficients between all features in each dataset, which yielded two correlation matrices of the same size. We then calculated the average of all cell-wise absolute differences between the two matrices to quantify the fidelity loss in a synthetic dataset. We multiplied all values by a factor of 1000² for presentation purposes. For reference convenience, we name this quantity as correlation distance.

Latent cluster analysis. This measure assesses the deviation of a synthetic dataset in the underlying latent space from the corresponding real dataset in terms of an unsupervised clustering²⁷. For each pair of real and synthetic datasets, we stacked them into a larger dataset and reduced the dimensionality of the space by applying a principal component analysis (PCA) and retaining the dimensions that cover 80% of the variance in the system. We then applied K -means to define the clusters, where K was determined based on the elbow method (which was set to 3 for both datasets). The following clustering-based value was then calculated to quantify the deviation of synthetic data from real data:

$$\log \left(\frac{1}{K} \sum_{i=1}^K \left[\frac{n_i^R}{n_i} - 0.5 \right]^2 \right)$$

where n_i^R and n_i denote the number of real data points and the total number of data points in the i^{th} cluster, respectively. We name this quantity as latent deviation for reference convenience. For this metric, a lower value implies that the density functions of the real and synthetic datasets in the latent space are more similar.

Clinical knowledge violation. Unlike the previous metrics, this metric focuses on the record-level utility. Specifically, it quantifies the degree to which a generative model learns to synthesize clinically meaningful

records in terms of the ability to capture clinical knowledge from data. An example for continuous features is that the systolic blood pressure of a patient should be greater than the corresponding diastolic pressure. A synthetic dataset with a number of conflicts against clinical knowledge derived from real data can be less useful in those use cases that rely on record-level readability. In this study, we used a data-driven approach to derive the clinical knowledge from real data for model evaluation. We first identified the phecodes from real data that were only associated with one gender. For each gender, we then selected the most prevalent three phecodes that were only associated with this gender in real data. For each synthetic dataset, we computed the odds of each selected phecode appearing in the opposite gender. The average value from the selected phecodes was then calculated, where a higher value implies a lower capability of representing the clinical knowledge inherent in the real data.

Prediction Performance and important features. One of the more common scenarios for which synthetic EHR data is expected to provide support is machine learning model development and evaluation^{57,58}. To assess this capability, we performed two types of analysis. The first, which is straightforward and has been widely utilized, compares model performance for a specific prediction task in two distinct scenarios: (1) training a machine learning model using the synthetic dataset (obtained from a generative model learned from a real dataset) and then perform an evaluation based on an independent real dataset, and (2) training a model based on the independent real dataset and evaluate it using the synthetic dataset. In each scenario, for comparison purposes, the reference model is trained based on the corresponding real dataset. The first scenario adheres to how the synthetic data will be utilized after data are shared in practice. By contrast, the second plays a complementary role in that it assesses how convincingly the synthetic records match their labels²⁸. It should be noted that, in the second scenario, it is possible that the testing performance for certain synthetic data is higher than for the real data because of the potential of mode collapse for GAN models (which means a generative model can only generate synthetic records that are close to a subset of real data). However, we do not believe this is a concern, due to the fact that the other utility metrics will reflect this problem in the final model ranking.

For prediction, we applied light gradient boosting machines (LightGBMs) due to their consistent superior performance over traditional machine learning models in healthcare⁵⁹⁻⁶¹. In this evaluation, we randomly partitioned each real dataset according to a 70:30 split, where the 30% data served as the independent real dataset. We use the area under the receiver operating characteristic curve (AUROC) as the performance measure. We used bootstrapping to derive a 95% confidence interval for each model.

The second analysis focuses on the degree to which a synthetic dataset provides reliable insights into important features in the prediction task. This was incorporated as a critical metric because model explainability is critical for engendering trust and conducting algorithmic audits^{62,63}. To do so, we counted the shared top important features for models trained on a synthetic dataset and the corresponding real dataset. We used the SHapley Additive exPlanations (SHAP)⁶⁴ value to rank features and defined the important features as the top M features that retain 90% of the performance on real data, which was 20 and 25 for the VUMC and UW datasets, respectively.

Privacy

We focused on three types of privacy attacks that have targeted fully synthetic patient datasets: attribute inference²⁰, membership inference^{20,30}, and meaningful identity disclosure²⁹. In an attribute inference attack, given the synthetic dataset and partial information (e.g., demographics and phenotypic attributes) of a patient's record in the real dataset, an adversary can infer all sensitive attributes of the record. Henceforth, we use "real dataset" to denote "real training dataset" for simplicity. In a membership inference attack, given the synthetic dataset and a patient's record, an adversary can infer whether the patient's record is in the real dataset, which discloses sensitive information shared by all records in the real dataset (e.g., an HIV-positive dataset). In a meaningful identity disclosure attack, given the synthetic dataset and a population dataset with identifiers, an adversary can infer the identity (and sensitive attributes) of a patient's record in the real dataset by matching an identified record to a record in the synthetic dataset which also matches a

record in the real dataset due to potential overfitting of the data generation process. In general, among the three attacks, a larger number of attributes (i.e., identities and sensitive attributes) can be inferred for each victim in the meaningful identity disclosure attack, whereas a smaller number of attributes (i.e., membership) can be inferred for each victim in the membership inference attack.

Attribute inference. In an attribute inference attack²⁰, an adversary attempts to infer a set of sensitive attributes of a targeted record in the real dataset given a set of the targeted record's attributes and the synthetic dataset. The set of attributes known by the adversary usually includes demographic attributes, such as age, gender, or race⁶⁵. Sometimes, the adversary also knows the target's common clinical phenomena such as a diagnosis of the flu, cold, stomach ache, or conjunctivitis. In these cases, the sensitive attributes correspond to the target's other diseases. We assume the adversary attempts to infer the attributes using a k -nearest neighbors (KNN) algorithm. More specifically, the adversary first finds the set of k records in the synthetic dataset that are the most similar to the targeted record based on the set of known attributes as the neighbors. Given this set, the adversary attempts to infer each unknown attribute using a majority rule classifier for the members in the set.

To evaluate the attribute inference risk, we first calculated the inference risk for each attribute that the adversary wants to infer for a set of patient records. For each binary attribute, we simulated the inference attack and calculated the F1 score. Each categorical attribute was converted into binary attributes using one-hot coding. For each continuous attribute, we simulated the inference attack and calculated the accuracy, which is defined as the rate that the prediction is sufficiently close to the true value according to a closeness threshold. Afterwards, we set the attribute inference risk measure as a weighted sum of the risks for attributes, where the weight for each attribute is proportional to the corresponding information entropy in the real dataset and all weights sum to one.

We used the entire real dataset as the set of targeted records. In the KNN algorithm, we set k to 1 and use the Euclidean distance measure. We assumed that the adversary knows the demographic attributes (age, gender, and race for the VUMC dataset; gender, and race for the UW dataset) and the 256 phecodes that are most frequent in the real dataset. The adversary attempts to infer all of the other phecodes and numerical attributes. In this study, the closeness threshold was set to 0.1. In two supplementary experiments, we varied the setting by changing k to 10 or changing the number of known phecodes to 1024.

Membership inference. Knowing that an individual corresponds to a record in the real dataset constitutes a privacy risk because the records may be included according to specific criteria. For instance, these criteria may be disease- (e.g., HIV) or lifestyle-dependent (e.g., a certain sexual orientation). Notably, this information may not be included as an attribute in the real dataset because it is shared by all records in the dataset (e.g., when all of the real records select for their HIV positive status) and, thus, cannot be inferred in the aforementioned attribute inference attack. The adversary, with the knowledge of all or partial attributes of a target, can infer the membership by comparing the targeted record to all records in the synthetic dataset on those known attributes. A correct inference would reveal the target's sensitive information and also discredit the data sharer who aimed not to reveal that a certain individual was in the training data.

To evaluate the membership inference risk²⁰, we assume that the adversary is in possession of all attributes of a set of targeted records and we know whether each targeted record is in the real dataset. We first calculate the Euclidean distance between each synthetic record and each targeted record in terms of all attributes. Given a distance threshold, the adversary claims that a targeted record is in the real dataset if there exists at least one record with a distance smaller than the threshold. After the adversary infers the membership status of the targeted records, the F1 score of the membership inference would be used as the risk measure.

We use all records in the real dataset and the evaluation dataset as the targeted records. We normalize all continuous attributes into a range of zero and one. We set the distance threshold to 2 in the main experiment and 5 in the supplementary experiment to assess the sensitivity of the model.

Meaningful identity disclosure. Although a fully synthetic dataset appears to have no risk of identity disclosure, a synthetic dataset generated by an overfitted machine learning model may permit record linkage to the original records. In recognition of this fact, El Emam et al. introduced a risk model²⁹ that considers both identity disclosure and the ability of an adversary to learn new information upon doing so. In this attack, the adversary links the synthetic dataset to a population dataset, which is an identified dataset that covers the underlying population of the real dataset, upon quasi-identifiers (i.e., the common attributes in both datasets). Afterwards, for each targeted record in the synthetic dataset, the adversary infers the identity using a majority classifier over the linked records in the population dataset. They further assumed that the adversary can execute the record linkage attack by generalizing any attribute in any record to a certain level (i.e., an age, 20, can be generalized to an age group, [20 - 29]).

To evaluate the meaningful identity disclosure risk²⁹, we use the metric introduced by El Eman et al., which is based on the marketer risk measure⁶⁶ and additionally considers the uncertainty and errors in the adversary's inference. This metric is calculated as:

$$\max \left(\frac{1}{N} \sum_{s=1}^n \left(\frac{1}{f_s} \times \frac{1 + \lambda_s}{2} \times I_s \times R_s \right), \frac{1}{n} \sum_{s=1}^n \left(\frac{1}{F_s} \times \frac{1 + \lambda_s}{2} \times I_s \times R_s \right) \right),$$

where N is the number of records in the population, s is the index for a record in the real dataset. n is the number of records in the real dataset, f_s is the number of records in the real dataset that can match record s in the real dataset in terms of values on the quasi-identifiers (QIDs), F_s is the number of records in the population that can match record s in the real dataset in terms of values on the QIDs, λ_s is an adjustment

factor based on error rates sampled from 2 triangular distributions²⁹, I_s is a binary indicator of whether record s in the real dataset matches a record in the synthetic dataset, R_s is a binary indicator of whether the adversary would learn something new, and R_s is 1 if at least $L\%$ of the sensitive attributes satisfy the following criteria. For each categorical attribute, the criteria are: (1) there is at least one synthetic record that can match at least one real record on that sensitive attribute, and (2) $p_j < 0.5$, in which p_j is the proportion in the real sample that have the same j value, and $j \in J$ in which J is the set of different values the sensitive feature can take. For each continuous attribute, the criterion is $p_s \times |X_s - Y_t| < 1.48 \times MAD$, in which p_s is the proportion in the real sample that are in the same cluster with the real record after a univariate k -means clustering, X_s is the sensitive attribute of the real record, Y_t is the sensitive attribute of the synthetic record matching the real record, and MAD is the median absolute deviation.

In this study, we rely upon an adversarial model that is as strong as the one introduced by El Eman et al.²⁹ (i.e., with a similar sample-to-population ratio and a similar number of QIDs). For the VUMC dataset, we assume that the adversary has access to a population dataset of 633,035 records, which includes the name and 10 QIDs of all patients that have visited VUMC before February 2021. The corresponding QIDs are three demographic attributes (namely, age, sex, and race) and seven phenotypic attributes that are the most frequent diseases of those patients. For the UW dataset, we assume that the adversary has access to a population dataset of 466,980 records including the name and 10 QIDs of all patients who have visited UW at least five times in the past two years prior to the index event date, which is defined as the date of the latest recorded visit as of February 2019. The corresponding QIDs are two demographic attributes (namely, sex and race) and eight phenotypic attributes that are the most frequent diseases of those patients. The parameter L is set to 1 which means at least 26 (or 27) attributes need to be inferred correctly and meaningfully for an attack to be regarded as a successful attack that brings risk to VUMC (or UW) dataset. The difference between VUMC and UW datasets is due to the fact that the VUMC dataset has 74 fewer

attributes than the UW dataset. To test the sensitivity of the model, we change the parameter setup by changing L to 0.1 in the supplementary experiment.

Ranking mechanism

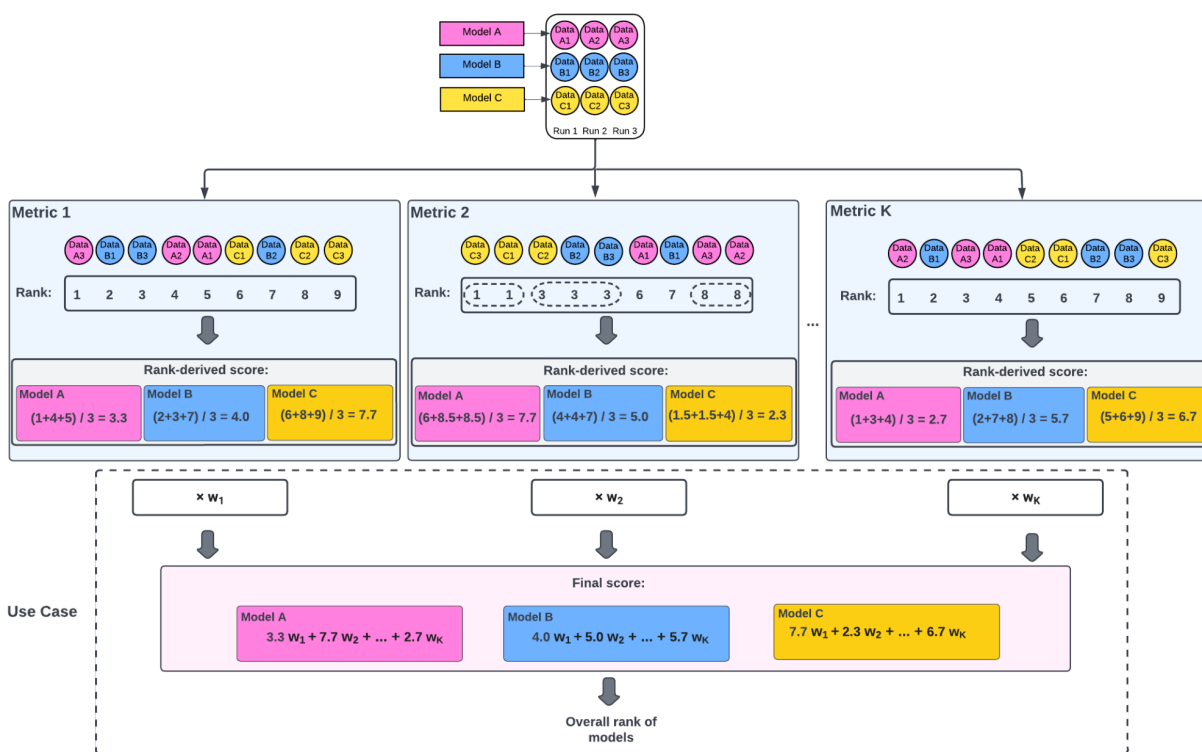


Figure 7. An illustration of the ranking mechanism of the benchmarking framework. The ovals with dashed edges indicate the ties in ranks. To calculate the rank-derived score for each model regarding Metric 2, datasets C3 and C1 tied for the rank of 1 and are assigned with the same adjusted rank of 1.5 in the calculation. In the same manner, datasets C2, B2, and B3 tied for the rank of 3 and are assigned with the same adjusted rank of 4 in the calculation.

Fig. 7 provides a concrete example of how our benchmarking framework ranks models. In this example, we use three candidate synthesis models to illustrate the process. When ranking models, with respect to each metric, each model receives a rank-derived score that is calculated as the average of ranks of three datasets associated with each model. The final score for each model is calculated as the weighted sum of the rank-derived scores from all metrics. All models are then ranked according to their final scores.

When ranking datasets, ties (i.e., two or more datasets having exactly the same value of a metric) can occur. In this case, the datasets receive the same adjusted rank (which is not necessarily an integer). In the example, there are three datasets that are tied in terms of an evaluation metric (Metric 2 in Fig. 7). The associated indices are 3, 4, and 5. The average of these three indices is thus $(3 + 4 + 5)/3 = 4$, which is taken as the adjusted rank that each of the three datasets would be assigned.

Use case description

In this study, we consider three use cases of synthetic data to demonstrate generative model selections in the context of specific needs. The benchmarking framework translates a use case into weights on the metric-level results. By default, a weight of 0.1 was assigned to each metric, and all weights sum to 1. We adjusted the weights according to the needs of the use case. The following provides a summary of the use case, while the detailed weight profiles are provided in Supplementary Table C.1.

Education. It is expected that synthetic EHR data will support educational purposes. The potential data users for this use case are students interested in health informatics or entry-level health data analytics. In general, privacy risks in this use case are relatively small for several reasons: 1) access control and audit logs are easy to implement, and 2) data use agreement can be applied to further protect the data. By contrast, the educational use case has high demand in maintaining the statistical characteristics of the real medical records and minimizing obvious clinical inconsistencies. Thus, we lowered the weight assigned to each of the privacy metrics to 0.05 and raised the weight for dimensional-wise distribution to 0.25, column-wise correlation, and clinical knowledge violation to 0.15, with the remaining metrics set to 0.1.

Medical AI development. It has been repeatedly shown that synthetic health data are able to support the development of medical AI by providing similar testing performance as on real data^{10,67,68}. We established the use case for machine learning model development based on the aforementioned prediction tasks: 1) 21-

day hospital admission post positive COVID-19 testing (for the VUMC dataset) and 2) six-month mortality (for the UW dataset). In this use case, we prioritized the model prediction-related utility metrics (performance results and feature selection) and privacy because the synthetic data are open to the broad data science community. As such, we raised the combined privacy weight to 0.3 and model performance to 0.5.

System development. In the healthcare domain, software systems development teams often need access to sufficiently large and realistic datasets that mimic real data for function and workflow testing, as well as computational resource estimation. In this use case, it is important that the synthetic data maintain both the size and the sparsity of the real data. These are factors represented in metrics for dimension-wise distribution. At the same time, privacy needs to be prioritized as the engineers may not have the right to work with the records of patients - particularly if they are not employees of the healthcare organization. Thus, we set the dimension-wide distribution weight to 0.25, the privacy metrics to 0.5, while the rest of the weights were set to 0.05.

Synthesis paradigms

In this study, we investigated two common synthesis paradigms as examples. The first strategy treats the outcome variable the same as other features in model training, which leads to a *combined* synthesis paradigm (Fig. 6C), whereas the second strategy was designed to independently train a generative model for each outcome represented by the outcome variable, leading to a *separate* synthesis paradigm (Fig. 6D). It should be noted that data synthesis paradigms are considered orthogonal to candidate generative models and use cases, and are embedded into the Synthetic EHR data generation phase.

We applied the combined synthesis paradigm to both datasets and all results that have been communicated so far were based on this strategy. We performed a comparison between the two strategies on the UW dataset. We did not conduct the comparison for the VUMC dataset because the volume of positive records

is too small to support separate GAN training. We ensured that the synthesized data shared the same size as the corresponding real dataset and that the distribution of the outcome variable remained the same as well.

More specifically, for each metric in the Multifaceted assessment phase, the number of synthetic datasets for evaluation becomes $n_m \times n_d \times n_s$, where n_m , n_d , and n_s denote the number of candidate generative models for benchmarking, the number of synthetic datasets considered for each model in comparison, and the number of considered synthesis paradigms, respectively. In this investigation, we have $6 \times 3 \times 2 = 36$ synthetic datasets for the UW dataset.

DATA AVAILABILITY

The data that support the findings of this study are available upon request from the corresponding authors and approval from the institutions' respective IRBs.

CODE AVAILABILITY

The source code associated with this study is publicly available at: <https://github.com/yy6linda/synthetic-ehr-benchmarking>.

ACKNOWLEDGEMENTS

This study was supported by NIH grants UL1TR002243, UL1TR002319, P30AR072572, and P50AG005136.

AUTHOR CONTRIBUTIONS

C.Y., Y.Y., and Z.W. contributed to the conception and design of the study. C.Y., Y.Y., Z.W., and Z.Z. conducted the analysis and interpreted the results. C.Y., Y.Y., and Z.W. led the writing of the manuscript and are co-first authors. B.A.M, L.O., J.G., and S.M. revised the manuscript. B.A.M. and S.M. supervised the research. All authors helped shape the research, analysis, and manuscript. All authors wrote the manuscript. All authors read and approved the final manuscript.

COMPETING INTERESTS

All authors have no competing interests to declare.

REFERENCES

1. Tresp, V. *et al.* Going Digital: A Survey on Digitalization and Large-Scale Data Analytics in Healthcare. *Proc. IEEE* **104**, 2180–2206 (2016).
2. Topol, E. J., Steinhubl, S. R. & Torkamani, A. Digital medical tools and sensors. *JAMA* **313**, 353–354 (2015).
3. Elenko, E., Underwood, L. & Zohar, D. Defining digital medicine. *Nat. Biotechnol.* **33**, 456–461 (2015).
4. Packer, M. Data sharing in medical research. *BMJ* **360**, k510 (2018).
5. Wirth, F. N., Meurers, T., Johns, M. & Prasser, F. Privacy-preserving data sharing infrastructures for medical research: systematization and comparison. *BMC Med. Inform. Decis. Mak.* **21**, 242 (2021).
6. El Emam, K., Rodgers, S. & Malin, B. Anonymising and sharing individual patient data. *BMJ* **350**, h1139 (2015).
7. Dinov, I. D. Methodological challenges and analytic opportunities for modeling and interpreting Big Healthcare Data. *GigaScience* **5**, s13742-016-0117-6 (2016).
8. Ghosheh, G., Li, J. & Zhu, T. A review of Generative Adversarial Networks for Electronic Health Records: applications, evaluation measures and data sources. *arXiv [cs.LG]* (2022).
9. Chen, R. J., Lu, M. Y., Chen, T. Y., Williamson, D. F. K. & Mahmood, F. Synthetic data in machine learning for medicine and healthcare. *Nat. Biomed. Eng.* **5**, 493–497 (2021).
10. Rankin, D. *et al.* Reliability of Supervised Machine Learning Using Synthetic Data in Health Care: Model to Preserve Privacy for Data Sharing. *JMIR Med. Inform.* **8**, e18910 (2020).
11. Foraker, R., Mann, D. L. & Payne, P. R. O. Are Synthetic Data Derivatives the Future of Translational Medicine? *JACC Basic Transl. Sci.* **3**, 716–718 (2018).
12. Haendel, M. A. *et al.* The National COVID Cohort Collaborative (N3C): Rationale, design, infrastructure, and deployment. *J. Am. Med. Inform. Assoc.* **28**, 427–443 (2021).
13. Wang, Z., Myles, P. & Tucker, A. H. Generating and evaluating cross-sectional synthetic electronic

- healthcare data: Preserving data utility and patient privacy. *Comput. Intell.* **37**, 819–851 (2021).
14. Hernandez, M., Epelde, G., Alberdi, A., Cilla, R. & Rankin, D. Synthetic data generation for tabular health records: A systematic review. *Neurocomputing* **493**, 28–45 (2022).
 15. Lan, L. *et al.* Generative Adversarial Networks and Its Applications in Biomedical Informatics. *Front Public Health* **8**, 164 (2020).
 16. Goodfellow, I. *et al.* Generative adversarial nets. *Adv. Neural Inf. Process. Syst.* **27**, (2014).
 17. McLachlan, S., Dube, K. & Gallagher, T. Using the CareMap with Health Incidents Statistics for Generating the Realistic Synthetic Electronic Healthcare Record. in *2016 IEEE International Conference on Healthcare Informatics (ICHI)* 439–448 (2016).
 18. Walonoski, J. *et al.* Synthea: An approach, method, and software mechanism for generating synthetic patients and the synthetic electronic health care record. *J. Am. Med. Inform. Assoc.* **25**, 230–238 (2018).
 19. Norel, R., Rice, J. J. & Stolovitzky, G. The self-assessment trap: can we all be better than average? *Mol. Syst. Biol.* **7**, 537 (2011).
 20. Zhang, Z., Yan, C., Mesa, D. A., Sun, J. & Malin, B. A. Ensuring electronic medical record simulation through better training, modeling, and evaluation. *J. Am. Med. Inform. Assoc.* **27**, 99–108 (2020).
 21. Yan, C., Zhang, Z., Nyemba, S. & Malin, B. A. Generating Electronic Health Records with Multiple Data Types and Constraints. *AMIA Annu. Symp. Proc.* **2020**, 1335–1344 (2020).
 22. Skandarani, Y., Lalande, A., Afilalo, J. & Jodoin, P.-M. Generative Adversarial Networks in Cardiology. *Can. J. Cardiol.* **38**, 196–203 (2022).
 23. Karras, T., Aila, T., Laine, S. & Lehtinen, J. Progressive Growing of GANs for Improved Quality, Stability, and Variation. *arXiv [cs.NE]* (2017).
 24. Rasmy, L., Xiang, Y., Xie, Z., Tao, C. & Zhi, D. Med-BERT: pretrained contextualized embeddings on large-scale structured electronic health records for disease prediction. *NPJ Digit. Med.* **4**, 86 (2021).
 25. Choi, E. *et al.* Generating Multi-label Discrete Patient Records using Generative Adversarial Networks. in *Proceedings of the 2nd Machine Learning for Healthcare Conference* (eds. Doshi-Velez,

- F. et al.) **68**, 286–305 (PMLR, 18--19 Aug 2017).
26. Goncalves, A. *et al.* Generation and evaluation of synthetic patient data. *BMC Med. Res. Methodol.* **20**, 108 (2020).
 27. Woo, M.-J., Reiter, J. P., Oganian, A. & Karr, A. F. Global Measures of Data Utility for Microdata Masked for Disclosure Limitation. *JPC J. Planar Chromatogr. - Mod. TLC* **1**, (2009).
 28. Esteban, C., Hyland, S. L. & Rätsch, G. Real-valued (Medical) Time Series Generation with Recurrent Conditional GANs. *arXiv [stat.ML]* (2017).
 29. El Emam, K., Mosquera, L. & Bass, J. Evaluating Identity Disclosure Risk in Fully Synthetic Health Data: Model Development and Validation. *J. Med. Internet Res.* **22**, e23139 (2020).
 30. Zhang, Z., Yan, C. & Malin, B. A. Membership inference attacks against synthetic health data. *J. Biomed. Inform.* **125**, 103977 (2022).
 31. Wang, K. *et al.* Generative adversarial networks: introduction and outlook. *IEEE/CAA Journal of Automatica Sinica* **4**, 588–598 (2017).
 32. Luo, Y., Zhu, L.-Z., Wan, Z.-Y. & Lu, B.-L. Data augmentation for enhancing EEG-based emotion recognition with deep generative models. *J. Neural Eng.* **17**, 056021 (2020).
 33. DuMont Schütte, A. *et al.* Overcoming barriers to data sharing with medical image generation: a comprehensive evaluation. *NPJ Digit. Med.* **4**, 141 (2021).
 34. Baowaly, M. K., Lin, C.-C., Liu, C.-L. & Chen, K.-T. Synthesizing electronic health records using improved generative adversarial networks. *J. Am. Med. Inform. Assoc.* **26**, 228–241 (2019).
 35. Xie, L., Lin, K., Wang, S., Wang, F. & Zhou, J. Differentially Private Generative Adversarial Network. *arXiv [cs.LG]* (2018).
 36. Bergquist, T. *et al.* Evaluation of crowdsourced mortality prediction models as a framework for assessing AI in medicine. *medRxiv* 2021.01.18.21250072 (2021).
 37. Agency, E. M. External guidance on the implementation of the European Medicines Agency policy on the publication of clinical data for medicinal products for human use. <https://www.ema.europa.eu/en/human-regulatory/marketing-authorisation/clinical-data->

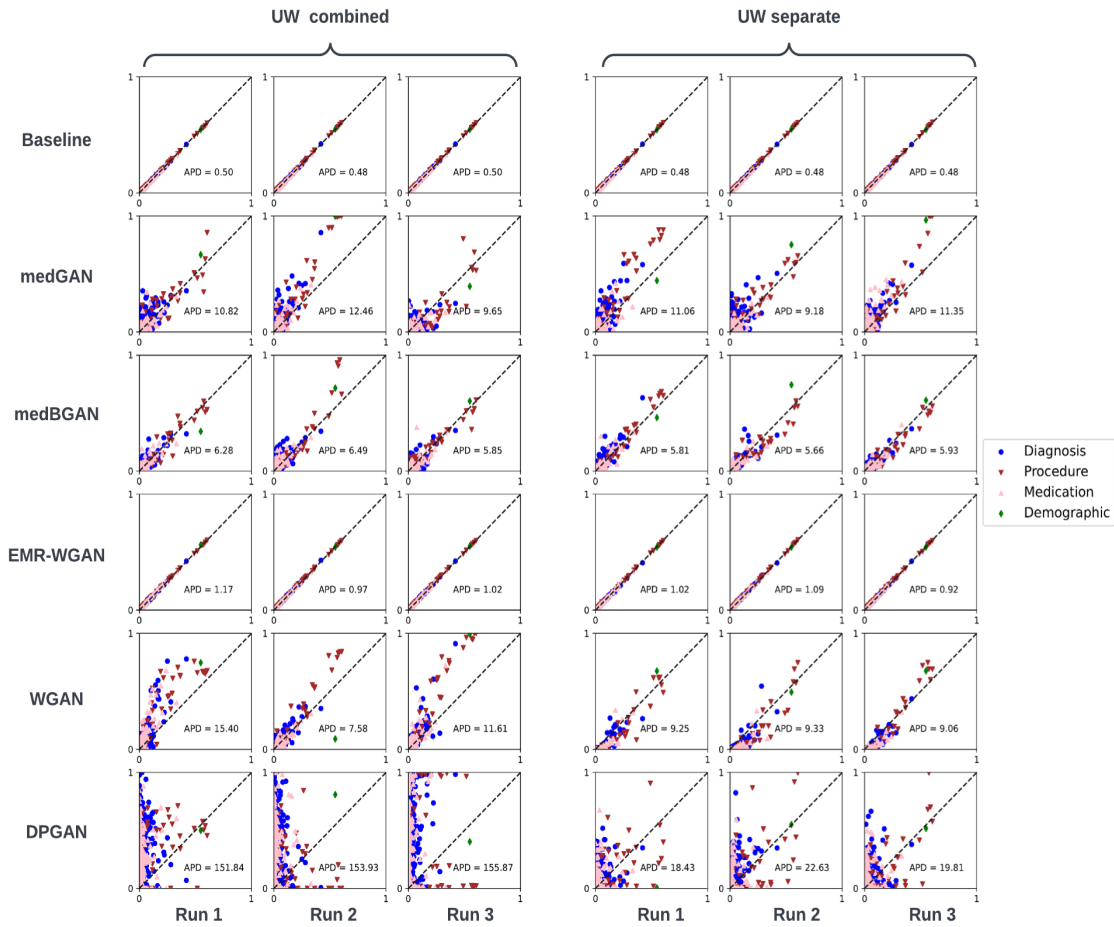
- publication/support-industry/external-guidance-implementation-european-medicines-agency-policy-publication-clinical-data (2018).
38. Health Canada. Public Release of Clinical Information: guidance document. <https://www.canada.ca/en/health-canada/services/drug-health-product-review-approval/profile-public-release-clinical-information-guidance/document.html> (2021).
 39. Bishop, A. Policy on protecting confidentiality in tables of birth and death statistics. <https://www.ons.gov.uk/methodology/methodologytopicsandstatisticalconcepts/disclosurecontrol/policyonprotectingconfidentialityintablesobirthanddeathstatistics> (2014).
 40. Centers for Disease Control and Prevention. Integrated guidance for developing epidemiologic profiles HIV prevention and Ryan white HIV/AIDS programs planning august 2014. <https://stacks.cdc.gov/view/cdc/40072> (2014).
 41. Wan, Z. *et al.* Expanding Access to Large-Scale Genomic Data While Promoting Privacy: A Game Theoretic Approach. *Am. J. Hum. Genet.* **100**, 316–322 (2017).
 42. Wan, Z. *et al.* Using game theory to thwart multistage privacy intrusions when sharing data. *Sci. Adv.* **7**, eabe9986 (2021).
 43. Bellovin, S. M. *Privacy and Synthetic Datasets.* (SSRN, 2018). https://papers.ssrn.com/sol3/papers.cfm?abstract_id=3255766.
 44. Li, J., Cairns, B. J., Li, J. & Zhu, T. Generating Synthetic Mixed-type Longitudinal Electronic Health Records for Artificial Intelligent Applications. *arXiv [cs.LG]* (2021).
 45. Frid-Adar, M., Klang, E., Amitai, M., Goldberger, J. & Greenspan, H. Synthetic data augmentation using GAN for improved liver lesion classification. in *2018 IEEE 15th International Symposium on Biomedical Imaging (ISBI 2018)* 289–293 (2018).
 46. Yang, Y. *et al.* GAN-Based Semi-Supervised Learning Approach for Clinical Decision Support in Health-IoT Platform. *IEEE Access* **7**, 8048–8057 (2019).
 47. Che, Z., Cheng, Y., Zhai, S., Sun, Z. & Liu, Y. Boosting Deep Learning Risk Prediction with Generative Adversarial Networks for Electronic Health Records. in *2017 IEEE International*

- Conference on Data Mining (ICDM) 787–792 (2017).*
48. Waheed, A. *et al.* CovidGAN: Data Augmentation Using Auxiliary Classifier GAN for Improved Covid-19 Detection. *IEEE Access* **8**, 91916–91923 (2020).
 49. Camino, R., Hammerschmidt, C. & Radu State. Generating Multi-Categorical Samples with Generative Adversarial Networks. *arXiv [stat.ML]* (2018).
 50. Torfi, A. & Fox, E. A. COR-GAN: Correlation-capturing convolutional neural networks for generating synthetic healthcare records. *The Thirty-Third International Flairs Conference* (2020).
 51. Bergquist, T. *et al.* Piloting a model-to-data approach to enable predictive analytics in health care through patient mortality prediction. *J. Am. Med. Inform. Assoc.* **27**, 1393–1400 (2020).
 52. Yan, Y. *et al.* A Continuously Benchmarked and Crowdsourced Challenge for Rapid Development and Evaluation of Models to Predict COVID-19 Diagnosis and Hospitalization. *JAMA Netw Open* **4**, e2124946 (2021).
 53. Zhang, Z., Yan, C., Lasko, T. A., Sun, J. & Malin, B. A. SynTEG: a framework for temporal structured electronic health data simulation. *J. Am. Med. Inform. Assoc.* **28**, 596–604 (2021).
 54. CPT Hierarchy. http://medpricemonkey.com/cpt_hierarchy_list.
 55. Arjovsky, M., Chintala, S. & Bottou, L. Wasserstein generative adversarial networks. *Proceedings of the 34th International Conference on Machine Learning* **70**, 214-223 (2017).
 56. Dwork, C. Differential Privacy: A Survey of Results. in *Theory and Applications of Models of Computation* 1–19 (Springer Berlin Heidelberg, 2008).
 57. Foraker, R. E. *et al.* Spot the difference: comparing results of analyses from real patient data and synthetic derivatives. *JAMIA Open* **3**, 557–566 (2020).
 58. Guo, A. *et al.* The Use of Synthetic Electronic Health Record Data and Deep Learning to Improve Timing of High-Risk Heart Failure Surgical Intervention by Predicting Proximity to Catastrophic Decompensation. *Frontiers in Digital Health* **2**, 576945 (2020).
 59. Zoabi, Y., Deri-Rozov, S. & Shomron, N. Machine learning-based prediction of COVID-19 diagnosis based on symptoms. *NPJ Digit. Med.* **4**, 3 (2021).

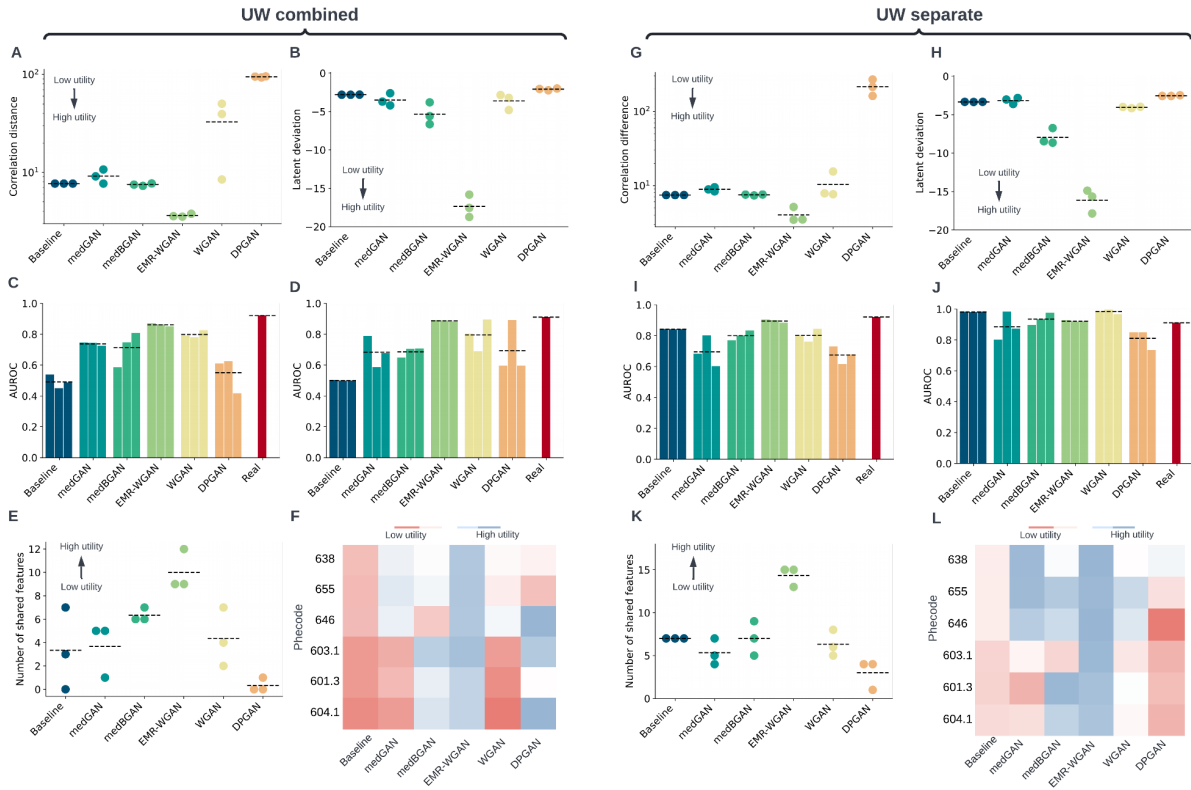
60. Artzi, N. S. *et al.* Prediction of gestational diabetes based on nationwide electronic health records. *Nat. Med.* **26**, 71–76 (2020).
61. Razavian, N. *et al.* A validated, real-time prediction model for favorable outcomes in hospitalized COVID-19 patients. *NPJ Digit. Med.* **3**, 130 (2020).
62. Liu, X. *et al.* The medical algorithmic audit. *Lancet Digit. Health* **4**, e384–e397 (2022).
63. Ghassemi, M., Oakden-Rayner, L. & Beam, A. L. The false hope of current approaches to explainable artificial intelligence in health care. *Lancet Digit. Health* **3**, e745–e750 (2021).
64. Lundberg & Lee. A unified approach to interpreting model predictions. *Adv. Neural Inf. Process. Syst.* **30** (2017).
65. Malin, B., Benitez, K. & Masys, D. Never too old for anonymity: a statistical standard for demographic data sharing via the HIPAA Privacy Rule. *J. Am. Med. Inform. Assoc.* **18**, 3–10 (2011).
66. Dankar, F. K. & El Emam, K. A method for evaluating marketer re-identification risk. in *Proceedings of the 2010 EDBT/ICDT Workshops* 1–10 (Association for Computing Machinery, 2010).
67. Tucker, A., Wang, Z., Rotalinti, Y. & Myles, P. Generating high-fidelity synthetic patient data for assessing machine learning healthcare software. *NPJ Digit. Med.* **3**, 147 (2020).
68. Foraker, R. *et al.* The National COVID Cohort Collaborative: Analyses of Original and Computationally Derived Electronic Health Record Data. *J. Med. Internet Res.* **23**, e30697–e30697 (2021).

Supplementary Information

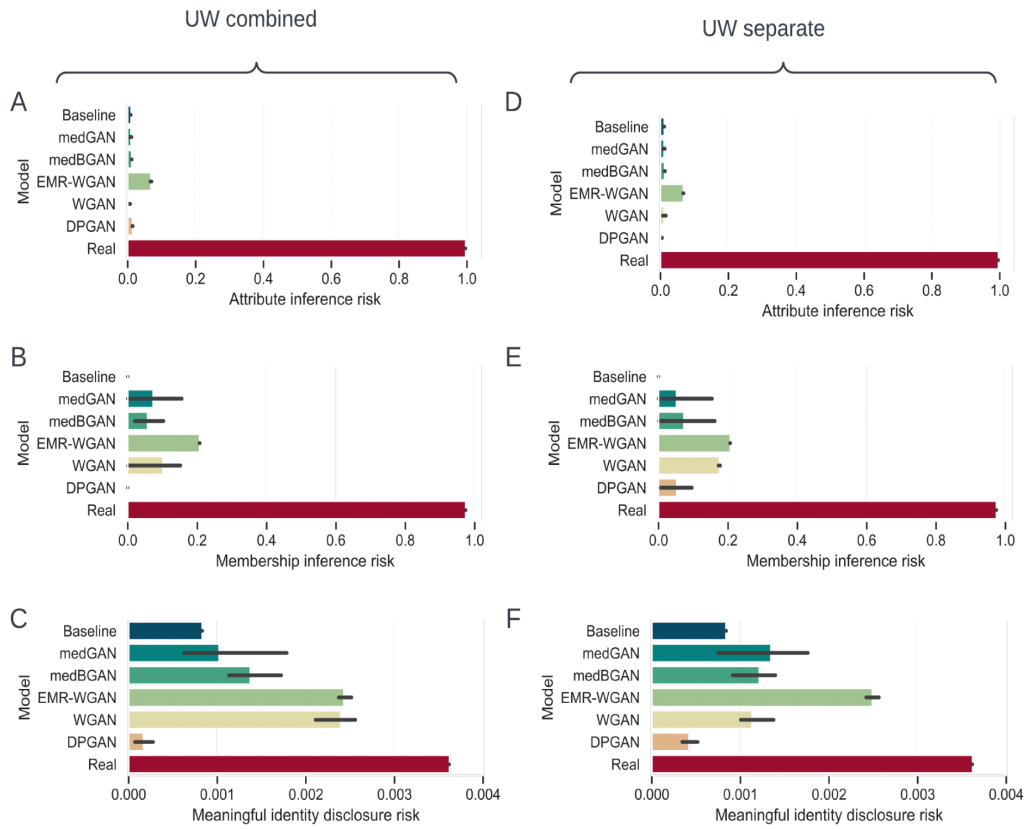
Supplementary A: Comparison of synthesis paradigms.



Supplementary Figure A.1 Dimension-wise distribution using a combined synthesis paradigm (left) and a separate synthesis paradigm (right) for the UW dataset. Here, the x- and y-axes correspond to the prevalence of a feature in real and synthetic data, respectively. The results for three independently generated synthetic datasets are shown for each candidate model. Feature dots on the dashed diagonal line correspond to the perfect replication of prevalence.



Supplementary Figure A.2 Data utility (except for dimension-wise distribution) from using separate synthesis paradigm (left, A-F) and combined synthesis paradigm (right, G-L) for the UW datasets. (A,G). Column-wise correlation, (B,H) Latent cluster analysis, (C,I) Model performance for training on synthetic data (trained from 70% real data) and testing on 30% real data, (D,J) Model performance for training on 30% real data and testing on synthetic data, (E,K) The number of top k features in common (k is 25 for UW and 20 for VUMC), (F,L) Clinical knowledge violation for gender-specific phecodes. Dashed lines indicate the mean values on multiple results. Log scale is applied to the y-axis in A and G. The heatmaps correspond to the ratio of clinical knowledge violations in gender (blue = low value; red = high value). A dashed line indicates the mean value across three synthetic datasets. (Phecode definitions: 638: Other high-risk pregnancy; 655: Known or suspected fetal abnormality; 646: Other complications of pregnancy NEC; 603.1: Hydrocele; 601.3: Orchitis and epididymitis; 604.1: Redundant prepuce and phimosis/BXO)



Supplementary Figure A.3 Average privacy risks of the synthetic datasets generated for the UW synthetic data using combined synthesis paradigm (A-C) and separate synthesis paradigm (D-F). (A,D) Attribute inference risk; (B,H) Membership inference risk; (C,I) Meaning identity disclosure risk. The risk associated with the real data is shown in the bottom red bars. The 95% confidence intervals are marked as thin horizontal black lines.

Supplementary Table A.1 The rank-derived scores for models with respect to the individual metrics using UW synthetic data generated under the separate synthesis paradigm. The best (i.e., lowest rank) and worst scores for each metric are marked as bold red and bold black, respectively.

Metric	Model					
	Baseline	medGAN	medBGAN	EMR-WGAN	WGAN	DPGAN
Dimension-wise distribution	2.0	13.3	8.0	5.0	11.7	17.0
Column-wise correlation	6.0	13.0	7.0	2.0	12.0	17.0
Latent cluster analysis	12.0	13.0	5.0	2.0	8.0	17.0
Model performance (TSTR)	6.0	14.0	10.2	2.0	9.2	15.7
Model performance (TRTS)	4.8	11.5	9.7	11.0	3.7	16.3
Feature selection	8.0	12.3	8.3	2.0	9.7	16.7
Clinical knowledge violation	14.0	8.0	6.0	2.0	10.0	17.0
Attribute inference	9.2	8.3	12.2	17.0	8.3	2.0
Member inference	3.0	5.7	8.7	17.0	14.0	8.7
Meaningful identity disclosure	6.0	11.0	10.7	17.0	10.3	2.0

Supplementary Table A.2 Overall rank of generative models for the use cases in the Model recommendation phase. Model ranks were based on the benchmarking framework scores (in parenthesis). The fact that medGAN and DPGAN have the same score in the System Development use case is due to precision loss instead of an actual tie.

Use case	Dataset	Final ranks of models					
		1	2	3	4	5	6
Education	UW separate	EMR-WGAN (5.0)	Baseline (7.0)	medBGAN (7.9)	WGAN (10.5)	medGAN (11.7)	DPGAN (14.9)
Medical AI Development	UW separate	EMR-WGAN (6.7)	Baseline (6.8)	medBGAN (9.3)	WGAN (10.0)	medGAN (11.6)	DPGAN (12.7)
System Development	UW separate	Baseline (5.8)	medBGAN (9.1)	EMR-WGAN (10.3)	medGAN (10.5)	DPGAN (10.5)	WGAN (10.8)

Supplementary Table A.3 Rank-derived scores for the UW synthetic datasets considering both the combined synthesis paradigm and separate synthesis paradigm. “_com” and “_sep” are used as suffix to denote the combined synthesis paradigm and the separate synthesis paradigm, respectively. The best (i.e., lowest rank) and worst scores for each metric are in bold red and black font, respectively.

	Baseline _com	Baseline _sep	medGA N_com	medGA N_sep	medBGA N_com	medBGA N_sep	EMR- WGAN_ com	EMR- WGAN_ sep	WGAN_ com	WGAN_ sep	DPGAN _com	DPGAN _sep
Dimension-wise distribution	4.0	3.0	26.0	24.7	16.7	14.3	9.8	9.2	25.7	21.7	35.0	32.0
Column-wise correlation	18.0	10.0	22.7	24.0	13.0	11.7	4.0	3.0	27.3	21.3	32.0	35.0
Latent cluster analysis	28.0	21.0	20.3	23.0	12.7	8.0	2.7	4.3	20.0	15.0	35.0	32.0
Model performance (TRTS)	35.0	4.8	28.7	15.2	27.7	9.7	16.7	<i>11.0</i>	21.3	3.7	26.3	22.0
Model performance (TSTR)	34.0	8.7	23.3	23.7	22.0	15.0	5.0	2.0	15.7	14.0	31.3	26.7
Feature selection	25.5	12.5	25.3	20.3	16.2	13.5	5.3	2.0	23.0	16.0	34.0	28.3
Clinical knowledge violation	31.7	28.0	20.7	17.3	11.0	13.7	2.3	5.3	24.7	21.0	11.7	34.7
Attribute inference	13.0	17.2	12.0	16.3	23.0	21.8	34.2	32.8	5.0	15.7	27.7	3.3
Membership inference	6.5	6.5	17.5	12.7	18.3	19.7	34.7	32.3	20.0	29.0	6.5	18.3
Meaningful identity disclosure	12.0	13.0	14.0	19.7	21.3	20.0	30.8	32.8	32.3	19.0	2.0	5.0

Supplementary Table A.4 Overall rank of generative models for the use cases in the Model recommendation phase using UW data under both separate and combined synthesis paradigms. Model ranks were based on the benchmarking framework scores (in parenthesis). “_com” and “_sep” are used as suffix to denote the combined synthesis paradigm and the separate synthesis paradigm, respectively.

Use case	Final ranks of models					
	1	2	3	4	5	6
Education	EMR-WGAN_sep (9.3)	EMR-WGAN_com (9.7)	Baseline_sep (12.5)	medBGAN_sep (14.1)	medBGAN_com (16.0)	Baseline_com (18.8)
Medical AI Development	Baseline_sep (11.7)	EMR-WGAN_sep (11.9)	EMR-WGAN_com (13.5)	medBGAN_sep (15.8)	WGAN_sep (17.6)	medBGAN_com (19.1)
System Development	Baseline_sep (10.9)	Baseline_com (13.1)	medBGAN_sep (16.9)	medBGAN_com (18.4)	medGAN_com (19.4)	EMR-WGAN_sep (19.5)

Use case	Final ranks of models					
	7	8	9	10	11	12
Education	WGAN_sep (19.5)	medGAN_sep (21.5)	medGAN_com (22.1)	WGAN_com (23.0)	DPGAN_com (27.1)	DPGAN_sep (28.5)
Medical AI Development	WGAN_com (19.6)	medGAN_sep (20.7)	medGAN_com (20.8)	DPGAN_sep (22.9)	Baseline_com (23.0)	DPGAN_com (25.4)
System Development	medGAN_sep (19.7)	EMR-WGAN_com (20.0)	DPGAN_sep (20.3)	WGAN_sep (20.4)	WGAN_com (21.5)	DPGAN_com (22.0)

Supplementary B: Detailed results for evaluation metrics.

Supplementary Table B.1 Results for dimension-wide distribution. The value is absolute prevalence rate difference (APD) for UW and combination of APD and average of the variable-wise Wasserstein distances (AWD) for VUMC.

		Baseline	medGAN	medBGAN	EMR-WGAN	WGAN	DPGAN
UW (combined)	Run_1	0.496	10.818	6.283	1.165	15.397	151.839
	Run_2	0.477	12.464	6.488	0.969	7.581	153.927
	Run_3	0.497	9.654	5.845	1.018	11.606	155.866
UW (separate)	Run_1	0.481	11.056	5.812	1.018	9.250	18.426
	Run_2	0.481	9.178	5.658	1.091	9.330	22.635
	Run_3	0.480	11.350	5.934	0.920	9.065	19.810
VUMC	Run_1	2.487	16.638	11.845	3.122	4.703	16.231
	Run_2	2.481	18.024	11.795	4.557	3.625	13.979
	Run_3	2.479	14.047	12.263	5.686	3.161	14.152

Supplementary Table B.2 Results for column-wise correlation.

		Baseline	medGAN	medBGAN	EMR-WGAN	WGAN	DPGAN
UW (combined)	Run_1	7.686	9.106	7.497	3.573	50.189	95.029
	Run_2	7.685	10.703	7.713	3.534	8.462	93.027
	Run_3	7.686	7.684	7.281	3.780	39.406	95.493
UW (separate)	Run_1	7.429	8.863	7.568	5.141	7.843	268.623
	Run_2	7.433	8.340	7.553	3.481	15.454	161.342
	Run_3	7.437	9.495	7.352	3.456	7.632	213.637
VUMC	Run_1	20.277	19.522	19.184	11.884	14.569	18.835
	Run_2	20.275	19.138	18.117	12.008	12.432	18.186
	Run_3	20.276	18.500	18.195	12.441	11.437	18.977

Supplementary Table B.3 Latent deviation for latent cluster analysis.

		Baseline	medGAN	medBGAN	EMR-WGAN	WGAN	DPGAN
UW (combined)	Run_1	-2.816	-3.712	-5.602	-18.736	-3.216	-2.000
	Run_2	-2.815	-2.614	-3.804	-17.547	-4.810	-2.235
	Run_3	-2.800	-4.196	-6.650	-15.822	-2.848	-2.059
UW (separate)	Run_1	-3.345	-3.025	-8.638	-15.647	-3.989	-2.568
	Run_2	-3.332	-3.613	-6.735	-14.880	-4.151	-2.465
	Run_3	-3.327	-2.828	-8.459	-17.848	-3.962	-2.568
VUMC	Run_1	-2.485	-2.592	-3.874	-16.860	-10.540	-2.680
	Run_2	-2.486	-2.531	-12.437	-12.141	-10.067	-2.588
	Run_3	-2.484	-6.846	-8.888	-9.344	-11.594	-6.132

Supplementary Table B.4 Results for model performance metrics.

Supplementary Table B.4.1a Model performance results for training on UW synthetic data generated using combined synthesis paradigm and testing on UW real data (TSTR). In contrast, training on 70% UW real data and testing on 30% UW real data lead to AUC 0.921 [0.916,0.926].

UW combined	Run_1	Run_2	Run_3	Overall
Baseline	0.537 [0.523,0.553]	0.449 [0.435,0.463]	0.486 [0.473,0.500]	0.491 [0.438,0.548]
medGAN	0.745 [0.733,0.757]	0.742 [0.731,0.753]	0.724 [0.713,0.735]	0.737 [0.716,0.754]
medBGAN	0.585 [0.571,0.599]	0.746 [0.734,0.757]	0.807 [0.797,0.817]	0.713 [0.575,0.814]
EMR-WGAN	0.870 [0.863,0.878]	0.862 [0.854,0.871]	0.851 [0.842,0.859]	0.861 [0.845,0.876]
WGAN	0.790 [0.778,0.801]	0.779 [0.768,0.790]	0.825 [0.816,0.834]	0.798 [0.771,0.832]
DPGAN	0.610 [0.596,0.625]	0.625 [0.614,0.636]	0.417 [0.405,0.429]	0.550 [0.408,0.634]

Supplementary Table B.4.1b Model performance results for training on UW synthetic data generated using separate synthesis paradigm and testing on UW real data (TSTR). In contrast, training on 70% UW real data and testing on 30% UW real data leads to AUC 0.921 [0.916,0.926].

UW separate	Run_1	Run_2	Run_3	Overall
Baseline	0.842 [0.833,0.851]	0.841 [0.831,0.850]	0.842 [0.833,0.851]	0.842 [0.832,0.851]
medGAN	0.682 [0.669,0.693]	0.801 [0.792,0.811]	0.602 [0.590,0.613]	0.695 [0.594,0.808]
medBGAN	0.769 [0.759,0.779]	0.799 [0.789,0.810]	0.833 [0.823,0.843]	0.800 [0.761,0.840]
EMR-WGAN	0.904 [0.898,0.910]	0.899 [0.892,0.905]	0.883 [0.876,0.890]	0.895 [0.878,0.908]
WGAN	0.799 [0.789,0.808]	0.760 [0.750,0.771]	0.843 [0.835,0.852]	0.801 [0.752,0.849]
DPGAN	0.729 [0.719,0.740]	0.617 [0.605,0.629]	0.677 [0.667,0.687]	0.674 [0.608,0.737]

Supplementary Table B.4.2a Model performance results for training on UW real data and testing on UW synthetic data generated using combined synthesis paradigm. In contrast, training on 30% UW real data and testing on 70% UW real data lead to AUC 0.911 [0.907,0.915].

UW combined	Run_1	Run_2	Run_3	Overall
Baseline	0.503 [0.495,0.511]	0.497 [0.489,0.506]	0.498 [0.490,0.506]	0.500 [0.491,0.509]
medGAN	0.788 [0.781,0.795]	0.587 [0.579,0.594]	0.676 [0.668,0.684]	0.684 [0.581,0.793]
medBGAN	0.647 [0.640,0.655]	0.704 [0.697,0.711]	0.706 [0.698,0.713]	0.686 [0.642,0.712]
EMR-WGAN	0.891 [0.887,0.895]	0.889 [0.884,0.893]	0.881 [0.877,0.885]	0.887 [0.877,0.894]
WGAN	0.802 [0.794,0.810]	0.689 [0.681,0.697]	0.894 [0.890,0.899]	0.795 [0.683,0.898]
DPGAN	0.595 [0.591,0.599]	0.890 [0.888,0.893]	0.595 [0.587,0.605]	0.693 [0.589,0.892]

Supplementary Table B.4.2b Model performance results for training on UW real data and testing on UW synthetic data generated using separate synthesis paradigm. In contrast, training on 30% UW real data and testing on 70% UW real data lead to AUC 0.911 [0.907,0.915].

UW separate	Run_1	Run_2	Run_3	Overall
Baseline	0.982 [0.980,0.983]	0.980 [0.978,0.981]	0.981 [0.980,0.983]	0.981 [0.979,0.983]
medGAN	0.800 [0.794,0.805]	0.982 [0.981,0.984]	0.874 [0.870,0.878]	0.885 [0.795,0.984]
medBGAN	0.896 [0.892,0.900]	0.934 [0.931,0.936]	0.975 [0.973,0.977]	0.935 [0.893,0.977]
EMR-WGAN	0.926 [0.923,0.929]	0.918 [0.915,0.921]	0.922 [0.919,0.925]	0.922 [0.916,0.928]
WGAN	0.987 [0.985,0.989]	0.996 [0.995,0.996]	0.966 [0.963,0.968]	0.983 [0.964,0.996]
DPGAN	0.849 [0.843,0.854]	0.848 [0.842,0.855]	0.734 [0.729,0.739]	0.810 [0.730,0.854]

Supplementary Table B.4.3 Model performance results for training on VUMC synthetic data and testing on VUMC real data. In contrast, training on 70% VUMC real data and testing on 30% VUMC real data leads to AUC 0.802 [0.772,0.830].

VUMC	Run_1	Run_2	Run_3	Overall
Baseline	0.617 [0.582,0.652]	0.575 [0.539,0.613]	0.500 [0.462,0.539]	0.564 [0.470,0.643]
medGAN	0.675 [0.640,0.706]	0.696 [0.662,0.731]	0.559 [0.523,0.598]	0.643 [0.532,0.722]
medBGAN	0.567 [0.530,0.606]	0.558 [0.518,0.596]	0.656 [0.618,0.691]	0.594 [0.527,0.685]
EMR-WGAN	0.717 [0.685,0.748]	0.728 [0.695,0.760]	0.691 [0.657,0.725]	0.712 [0.665,0.753]
WGAN	0.635 [0.596,0.669]	0.646 [0.612,0.680]	0.733 [0.696,0.767]	0.671 [0.605,0.757]
DPGAN	0.629 [0.593,0.667]	0.685 [0.652,0.716]	0.661 [0.625,0.693]	0.658 [0.602,0.709]

Supplementary Table B.4.4 Model performance results for training on VUMC real data and test on VUMC synthetic data. In contrast, training on 30% VUMC real data and testing on 70% VUMC real data lead to AUC 0.773 [0.752,0.796].

VUMC	Run_1	Run_2	Run_3	Overall
Baseline	0.508 [0.480,0.534]	0.502 [0.476,0.527]	0.499 [0.475,0.525]	0.503 [0.477,0.530]
medGAN	0.712 [0.689,0.734]	0.675 [0.653,0.696]	0.543 [0.518,0.571]	0.643 [0.524,0.728]
medBGAN	0.520 [0.495,0.546]	0.552 [0.532,0.573]	0.610 [0.583,0.637]	0.561 [0.502,0.630]
EMR-WGAN	0.691 [0.668,0.714]	0.724 [0.703,0.748]	0.634 [0.610,0.657]	0.683 [0.616,0.742]
WGAN	0.604 [0.581,0.629]	0.596 [0.571,0.620]	0.672 [0.649,0.695]	0.624 [0.577,0.689]
DPGAN	0.515 [0.492,0.537]	0.569 [0.544,0.594]	0.518 [0.493,0.542]	0.534 [0.494,0.586]

Supplementary Table B.5 Results for feature selection - number of top k features in common for models trained on synthetic data and real data separately. k is 25 for UW and 20 for VUMC.

		Baseline	medGAN	medBGAN	EMR-WGAN	WGAN	DPGAN
UW (combined)	Run_1	3	5	6	12	2	0
	Run_2	7	1	7	9	4	0
	Run_3	0	5	6	9	7	1
UW (separate)	Run_1	7	4	9	13	8	4
	Run_2	7	7	5	15	5	1
	Run_3	7	5	7	15	6	4
VUMC	Run_1	8	11	10	9	15	12
	Run_2	9	9	10	10	11	11
	Run_3	9	12	10	12	12	12

Supplementary Table B.6 Results for clinical knowledge violation.

Supplementary Table B.6.1 Clinical knowledge violation results for UW synthetic data using the combined synthesis paradigm.

UW combined	Run	Violation on female-only diseases			Violation on male-only diseases		
		638	655	646	603.1	601.3	604.1
Baseline	1	43.97%	43.95%	45.00%	52.95%	54.73%	57.76%
	2	44.27%	45.15%	44.32%	52.53%	53.79%	57.51%
	3	43.17%	46.31%	44.41%	57.11%	54.14%	59.17%
medGAN	1	8.74%	2.45%	9.49%	46.88%	21.72%	53.85%
	2	0.04%	0.05%	0.00%	99.60%	100.00%	100.00%
	3	50.22%	47.37%	47.33%	0.00%	13.15%	7.14%
medBGAN	1	33.72%	35.95%	47.56%	0.46%	4.76%	5.45%
	2	10.80%	9.64%	12.59%	15.71%	33.33%	25.81%
	3	25.30%	17.62%	60.88%	8.70%	17.24%	14.29%
EMR-WGAN	1	4.54%	4.95%	5.90%	2.85%	9.25%	8.75%
	2	5.33%	4.59%	5.15%	6.27%	6.72%	14.44%
	3	7.21%	6.56%	5.70%	0.74%	12.57%	5.40%
WGAN	1	2.26%	2.04%	7.26%	68.18%	88.75%	92.03%
	2	75.00%	87.84%	57.14%	4.60%	4.32%	6.25%
	3	0.00%	0.00%	0.00%	87.34%	80.22%	89.29%
DPGAN	1	15.09%	50.00%	0.00%	18.82%	33.56%	NAN
	2	17.30%	19.08%	NAN	0.00%	0.00%	0.00%
	3	51.39%	60.10%	NAN	0.00%	40.31%	0.00%

Supplementary Table B.6.2 Clinical knowledge violation results for UW synthetic data using the separate synthesis paradigm.

UW separate	Run	Violation on female-only diseases			Violation on male-only diseases		
		638	655	646	603.1	601.3	604.1
Baseline	1	45.44%	45.17%	45.30%	56.00%	55.30%	50.00%
	2	45.17%	44.20%	43.58%	51.47%	56.04%	52.71%
	3	44.19%	45.95%	45.35%	54.72%	51.55%	51.25%
medGAN	1	18.76%	19.26%	44.44%	25.35%	13.35%	0.00%
	2	0.65%	1.60%	0.17%	0.00%	92.11%	100.00%
	3	1.25%	0.59%	0.27%	99.59%	95.83%	NaN
medBGAN	1	60.35%	29.56%	38.61%	19.31%	2.20%	4.96%
	2	15.59%	4.55%	2.23%	70.00%	4.36%	29.72%
	3	31.90%	6.57%	23.65%	71.42%	11.54%	18.75%
EMR-WGAN	1	6.49%	6.06%	6.48%	8.42%	8.55%	9.46%
	2	3.94%	4.62%	4.84%	3.89%	8.10%	13.89%
	3	5.10%	8.61%	4.88%	6.09%	12.50%	10.34%
WGAN	1	30.00%	0.00%	21.21%	60.00%	44.44%	50.00%
	2	42.52%	36.67%	24.86%	34.62%	28.57%	30.70%
	3	41.55%	24.76%	33.33%	NaN	NaN	NaN
DPGAN	1	99.91%	99.62%	99.95%	0.10%	0.09%	0.11%
	2	0.00%	0.00%	92.41%	100.00%	100.00%	100.00%
	3	0.62%	NaN	66.67%	100.00%	87.47%	100.00%

Supplementary Table B.6.3 Clinical knowledge violation results for VUMC synthetic data.

VUMC	Run	Violation on female-only diseases			Violation on male-only diseases		
		625	614	792	796	601	185
Baseline	1	49.05%	44.93%	49.11%	60.00%	52.04%	50.47%
	2	48.50%	42.33%	43.58%	60.29%	52.07%	60.00%
	3	44.72%	41.34%	45.71%	60.16%	56.64%	57.61%
medGAN	1	6.69%	0.00%	5.83%	NaN	NaN	100.00%
	2	50.00%	87.50%	36.48%	1.43%	0.00%	0.00%
	3	2.52%	0.00%	50.00%	0.00%	0.00%	NaN
medBGAN	1	5.55%	21.27%	36.50%	35.71%	0.00%	33.33%
	2	14.29%	31.86%	50.00%	0.00%	7.41%	0.00%
	3	4.88%	37.69%	25.00%	42.86%	40.00%	50.00%
EMR-WGAN	1	8.73%	9.35%	10.82%	20.77%	9.38%	16.50%
	2	2.89%	9.62%	11.59%	15.79%	17.84%	23.21%
	3	8.08%	11.72%	6.44%	21.94%	16.67%	13.79%
WGAN	1	1.35%	6.22%	8.60%	14.94%	0.00%	20.59%
	2	6.26%	4.96%	3.59%	3.48%	7.55%	10.20%
	3	8.77%	9.25%	8.56%	5.21%	2.82%	9.86%
DPGAN	1	20.00%	33.33%	20.83%	66.66%	0.00%	100.00%
	2	17.39%	NaN	33.33%	36.76%	NaN	52.94%
	3	13.04%	22.72%	23.39%	0.00%	NaN	66.66%

Supplementary Table B.7 Results for attribute inference. k is the number of neighbors.

k	Known features	Data	Run	Baseline	medGA N	medBG AN	EMR- WGAN	WGAN	DPGAN	Real
1	256	UW (combined)	Run_1	0.00875	0.01096	0.01167	0.06611	0.00213	0.01344	0.99531
			Run_2	0.00865	0.00586	0.01166	0.06789	0.00319	0.01282	0.99531
			Run_3	0.00881	0.00659	0.01191	0.06986	0.00733	0.01447	0.99531
		UW (separate)	Run_1	0.01036	0.00689	0.01059	0.06611	0.01607	0.00193	0.99531
			Run_2	0.01044	0.01263	0.01300	0.06779	0.00752	0.00393	0.99531
			Run_3	0.01059	0.01008	0.01089	0.06782	0.00499	0.00432	0.99531
		VUMC	Run_1	0.09637	0.08594	0.08748	0.14969	0.12798	0.08031	0.99593
			Run_2	0.09687	0.08098	0.08511	0.14895	0.15233	0.10323	0.99593
			Run_3	0.09693	0.08848	0.09358	0.15233	0.14810	0.10233	0.99593
1	1024	UW (combined)	Run_1	0.00190	0.00064	0.00104	0.03075	0.00006	0.00163	0.99830
			Run_2	0.00201	0.00059	0.00102	0.03272	0.00004	0.00229	0.99830
			Run_3	0.00225	0.00071	0.00090	0.03253	0.00017	0.00224	0.99830
		UW (separate)	Run_1	0.00211	0.00033	0.00081	0.03113	0.00213	0.00005	0.99830
			Run_2	0.00204	0.00065	0.00082	0.03083	0.00030	0.00008	0.99830
			Run_3	0.00231	0.00068	0.00108	0.03239	0.00017	0.00009	0.99830
		VUMC	Run_1	0.19350	0.14313	0.15695	0.16574	0.13413	0.14044	0.99199
			Run_2	0.19327	0.14264	0.14056	0.16882	0.17658	0.18659	0.99199
			Run_3	0.19365	0.13977	0.15107	0.16250	0.17515	0.17253	0.99199
10	256	UW (combined)	Run_1	0.00000	0.00274	0.00216	0.02295	0.00004	0.01373	0.03992
			Run_2	0.00000	0.00121	0.00091	0.02368	0.00006	0.01275	0.03992
			Run_3	0.00000	0.00032	0.00113	0.02606	0.00093	0.01445	0.03992
		UW	Run_1	0.00000	0.00084	0.00045	0.02355	0.00160	0.00162	0.03992

		(separate)	Run_2	0.00000	0.00423	0.00144	0.02333	0.00130	0.00351	0.03992
			Run_3	0.00000	0.00155	0.00135	0.02299	0.00115	0.00274	0.03992
		VUMC	Run_1	0.08283	0.07314	0.05368	0.06544	0.07434	0.04725	0.13151
			Run_2	0.08373	0.04698	0.05636	0.07087	0.07069	0.07335	0.13151
			Run_3	0.08470	0.06802	0.05327	0.08959	0.06655	0.07682	0.13151

Supplementary Table B.8 Results for membership inference. θ is the threshold for the Euclidean distance between two records.

θ	Data	Run	Baseline	medGAN	medBGA N	EMR- WGAN	WGAN	DPGAN	Real
2	UW (combined)	Run_1	0.00000	0.15561	0.04662	0.20684	0.15168	0.00000	0.97374
		Run_2	0.00000	0.00000	0.01961	0.20726	0.14929	0.00000	0.97374
		Run_3	0.00000	0.06127	0.10261	0.20628	0.00012	0.00000	0.97374
	UW (separate)	Run_1	0.00000	0.00000	0.00021	0.20601	0.17738	0.09607	0.97374
		Run_2	0.00000	0.15449	0.05485	0.20619	0.17262	0.00159	0.97374
		Run_3	0.00000	0.00000	0.16172	0.20678	0.17525	0.05718	0.97374
	VUMC	Run_1	0.00000	0.22345	0.19321	0.27367	0.21279	0.00969	0.96428
		Run_2	0.00000	0.08140	0.24246	0.27683	0.19567	0.20762	0.96428
		Run_3	0.00000	0.19027	0.18375	0.27492	0.23326	0.00000	0.96428
5	UW (combined)	Run_1	0.00000	0.25168	0.18518	0.29654	0.25083	0.00000	0.95967
		Run_2	0.00000	0.00047	0.15972	0.29749	0.24937	0.00000	0.95967
		Run_3	0.00000	0.19955	0.20351	0.29572	0.02717	0.00000	0.95967
	UW (separate)	Run_1	0.00000	0.05134	0.13633	0.29583	0.27527	0.21971	0.95967
		Run_2	0.00000	0.24494	0.19329	0.29631	0.27258	0.11779	0.95967
		Run_3	0.00000	0.02205	0.25211	0.29643	0.27319	0.19553	0.95967
	VUMC	Run_1	0.00000	0.33593	0.33644	0.38220	0.34170	0.19587	0.94710
		Run_2	0.00000	0.28945	0.35799	0.38444	0.34812	0.33369	0.94710
		Run_3	0.00000	0.34026	0.31697	0.38250	0.36593	0.00569	0.94710

Supplementary Table B.9 Results for meaningful identity disclosure. θ is the ratio of the correctly inferred attributes in a successful attack.

θ	Data	Run	Baseline	medGAN	medBGA N	EMR- WGAN	WGAN	DPGAN	Real
0.001	UW (combined)	Run_1	0.00096	0.00317	0.00265	0.00353	0.00348	0.00026	0.00395
		Run_2	0.00096	0.00097	0.00307	0.00374	0.00376	0.00027	0.00395
		Run_3	0.00096	0.00223	0.00252	0.00357	0.00282	0.00050	0.00395
	UW (separate)	Run_1	0.00096	0.00312	0.00291	0.00371	0.00287	0.00092	0.00395
		Run_2	0.00096	0.00310	0.00205	0.00364	0.00223	0.00071	0.00395
		Run_3	0.00096	0.00145	0.00269	0.00373	0.00208	0.00088	0.00395
	VUMC	Run_1	0.00131	0.01402	0.01546	0.02359	0.01936	0.01209	0.04307
		Run_2	0.00132	0.00960	0.01357	0.02290	0.01727	0.01631	0.04307
		Run_3	0.00133	0.01032	0.01684	0.02528	0.02063	0.01126	0.04307
0.01	UW (combined)	Run_1	0.00083	0.00178	0.00126	0.00239	0.00256	0.00015	0.00362
		Run_2	0.00083	0.00062	0.00172	0.00251	0.00251	0.00007	0.00362
		Run_3	0.00083	0.00065	0.00113	0.00237	0.00211	0.00027	0.00362
	UW (separate)	Run_1	0.00083	0.00176	0.00139	0.00248	0.00137	0.00052	0.00362
		Run_2	0.00083	0.00151	0.00091	0.00242	0.00100	0.00034	0.00362
		Run_3	0.00084	0.00075	0.00132	0.00256	0.00101	0.00039	0.00362
	VUMC	Run_1	0.00110	0.00282	0.00734	0.01360	0.00940	0.00618	0.03817
		Run_2	0.00111	0.00310	0.00596	0.01357	0.01094	0.00948	0.03817
		Run_3	0.00109	0.00582	0.00953	0.01519	0.01285	0.00554	0.03817

Supplementary C: Metric weight profiles for use cases.

Supplementary Table C.1 Weight profiles for individual metrics for use cases. Note that in these use cases, we relied on TSTR results to characterize model utility in prediction performance.

Use case	Dimension-wide distribution	Column-wise correlation	Latent cluster analysis	Prediction performance	Feature selection	Clinical knowledge violation	Attribute inference	Membership inference	Meaningful identity disclosure
Education	0.25	0.15	0.1	0.1	0.1	0.15	0.05	0.05	0.05
Medical AI Development	0.05	0.05	0.05	0.35	0.15	0.05	0.1	0.1	0.1
Systems Development	0.25	0.05	0.05	0.05	0.05	0.05	1/6	1/6	1/6